



1985

In Partial Fulfillment of the
Requirements for the Degree of
Master of Science in Electrical Engineering

Roger L. Claypoole, Jr., BSEE
Captain, USAF

19941228 016

DEPARTMENT OF THE AIR FORCE
AIR UNIVERSITY
AIR FORCE INSTITUTE OF TECHNOLOGY

Wright-Patterson Air Force Base, Ohio

125 1250

AFIT/GE/ENG/94D-02

Multipoint Multirate Signal Processing

THESIS

Presented to the Faculty of the Graduate School of Engineering
of the Air Force Institute of Technology
Air Education and Training Command
In Partial Fulfillment of the
Requirements for the Degree of
Master of Science in Electrical Engineering

Roger L. Claypoole, Jr., BSEE
Captain, USAF

December, 1994

Approved for public release; distribution unlimited

Acknowledgements

I would like to thank my sponsor, Dr. Jon Sjogren of the Air Force Office of Scientific Research (AFOSR/NM). Special thanks go to my adviser, Dr. Bruce Suter, without whose help I would still be writing. His assistance, patience, and support went far beyond the call of duty. I would also like to thank my thesis committee, Dr. Michael Clark and Dr. Mark Oxley, for their patience and technical expertise.

Thanks go to all my fellow combatants in the Comm/Radar Laboratory. They helped to make my time at AFIT as enjoyable as possible.

Last but not least, I would like to thank my wife, Lisa, for her incredible support and understanding throughout the thesis writing process.

Roger L. Claypoole, Jr.

Accession For	
NTIS CRA&I	<input checked="checked" type="checkbox"/>
DTIC TAB	<input type="checkbox"/>
Unannounced	<input type="checkbox"/>
Justification _____	
By _____	
Date Issued / _____	
Availability Codes	
Dist	Avail and/or Special
A-1	

Table of Contents

	Page
Acknowledgements	ii
List of Figures	vi
Abstract	viii
 I. Introduction	 1
1.1 Problem Statement	1
1.2 Thesis Layout	2
 II. Background	 3
2.1 Comb Filters	3
2.2 Conventional Multirate Fundamentals	3
2.2.1 Definitions	3
2.2.2 z-Transforms of Building Blocks	4
2.2.3 Manipulation of Building Blocks	5
2.2.4 Polyphase Identities	6
2.3 Perfect Reconstruction Multirate Systems	8
2.4 Multiresolution Wavelet Decomposition and Multirate Sig- nal Processing	 11
2.4.1 Wavelet Decomposition Fundamentals	11
2.4.2 Relationship of the Wavelet Decomposition to Mul- tirate Signal Processing	 14
 III. Theoretical Foundations of Multipoint Multirate Signal Processing . .	 18
3.1 Fundamentals of Multipoint Multirate Signal Processing .	18
3.1.1 Definition of the Multipoint Decimator	18

	Page
3.1.2 z-transform Analysis of the Multipoint Decimator	19
3.1.3 Polyphase Analysis of the Multipoint Decimator .	21
3.1.4 Definition of the Multipoint Expander	23
3.1.5 z-transform Analysis of the Multipoint Expander	24
3.1.6 Polyphase Analysis of the Multipoint Expander .	26
3.1.7 Interconnections of Building Blocks	27
3.1.8 Multipoint Noble Identities	30
3.1.9 Multipoint Polyphase Representation	31
3.1.10 Conditions for Perfect Reconstruction in Multipoint Multirate Systems	32
3.1.11 Multipoint Polyphase Requirements for Perfect Re- construction	33
3.1.12 Design of Perfect Reconstruction Filter Banks using the Vector Polyphase Notation	41
3.2 Wavelet Decomposition with Multipoint Multirate Systems	47
IV. A Data Compression Feasibility Study	49
4.1 Introduction	49
4.2 Energy Redistribution Between Levels of the Multiresolution Analysis.	49
4.3 Summary	65
V. Conclusions and Recommendations for Further Study	67
5.1 Conclusions	67
5.2 Recommendations	67
Appendix A. The Multipoint Discrete Fourier Transform Matrix	69
Appendix B. Sufficient Conditions for Perfect Reconstruction in Multi- point Multirate Systems	74

	Page
Bibliography	81
Vita	83

List of Figures

Figure		Page
1.	Examples of Decimation and Expansion	4
2.	Fourier Representation of Decimation and Expansion	5
3.	Polyphase Representation	8
4.	M Channel Multirate Filter Bank	9
5.	M Channel Multirate System with Polyphase Matrices	10
6.	Multirate Implementation of the Multiresolution Wavelet Decomposition	17
7.	Examples of Multipoint Decimation and Expansion	19
8.	Equivalent Circuit for Multipoint Decimator	20
9.	Equivalent Circuit for Multipoint Expander	24
10.	Scaling a Decimated Sequence by a Scalar	28
11.	Adding Two Decimated Sequences	28
12.	Multiplying Two Decimated Sequences	29
13.	Multipoint Noble Identities	30
14.	Multipoint Polyphase Representation	32
15.	Multipoint System with Polyphase Matrix $P(z)$	34
16.	Multipoint Wavelet Decomposition Tree	47
17.	Daubechies Low Pass Filter D_8 for Various Vector Lengths	50
18.	Daubechies High Pass Filter D_8 for Various Vector Lengths	51
19.	Band Pass Signal and its Spectrum	52
20.	Energy Distribution for a Bandpass Signal	53
21.	Narrow Pass Signal and its Spectrum	55
22.	Energy Distribution for a Narrow Band Signal	56
23.	Sinusoid and its Spectrum	57
24.	Energy Distribution for a Sinusoid	57

Figure		Page
25.	Low Frequency Band Pass Signal and it Spectrum	58
26.	Energy Distribution for a Low Frequency Band Pass Signal	59
27.	High Pass Signal and its Spectrum	60
28.	Energy Distribution for a High Pass Signal	60
29.	Lenna	61
30.	Lenna's Eye	62
31.	Spectrum of Lenna's Eye	62
32.	Energy Distribution for Lenna's Eye	63
33.	Energy Distribution for Lenna's Eye with Zero Mean	64
34.	Bandpass Signal with Narrowband Features and its Spectrum	65
35.	Energy Distribution for Bandpass Signal with Narrowpass Features	66
36.	DFT Tree	72
37.	Partitioning of $P(z)$	75

Abstract

This thesis provides a fundamentally new, systematic study of multipoint multirate signal processing systems. The multipoint multirate operators are analyzed via equivalent circuits comprised entirely of conventional multirate operators. Interconnections of the operators are demonstrated, and the multipoint noble identities are derived. The multipoint polyphase representation is presented, and the M channel multipoint multirate system with vector length N is presented as an MN channel multipoint polyphase system.

The conditions sufficient for perfect reconstruction in the multipoint multirate system are derived. These conditions constrain the multipoint filter banks to be composed of comb filters generated from paraunitary sets of conventional filters. The perfect reconstruction multipoint multirate system is then combined with the multiresolution wavelet decomposition to form the generalized wavelet decomposition with varying vector decimation length at each level.

The generalized wavelet decomposition is used as an algorithm to redistribute the energy of a signal throughout the levels of the decomposition. It is shown that, for band pass and high pass signals, significant improvements can be made in the energy distribution. It is recommended that this algorithm be studied as a front end to a vector quantizer for data compression applications.

Multipoint Multirate Signal Processing

I. Introduction

1.1 Problem Statement

The study of multirate systems has advanced considerably in recent years. In particular, the basic building blocks have been explored [2], the conditions necessary for perfect reconstruction have been derived [13, 22, 19], and the relationship between multirate systems and the wavelet decomposition has been demonstrated [22, 19].

Recently, Khansari and Leon-Garcia have presented a few of the fundamentals of multirate systems with block sampling [6], or “multipoint multirate”. Meanwhile, vector transforms were introduced for image coding by Li [7, 8, 9], where input and output signals are finite length vectors of the same dimension. Li [7, 8, 9] has shown that these vector transforms have an advantage for image coding at low bit rates, because the local correlation between samples can be exploited more optimally when block signals are used.

Subsequently, being motivated by both the theoretical arguments of Khansari and Leon-Garcia and the practical arguments of Li, Suter and Xia have completed a more systematic presentation of vector filter banks [23], vector sampling [23], and vector wavelets [16]. However, there is still more research to be done in the area of multipoint multirate. This work presents new insights by providing a systematic study for relating multipoint multirate signal processing systems to conventional multirate signal processing systems. In addition, no work prior to this research has explored the idea of varying vector lengths at different levels of the multiresolution wavelet decomposition.

Thus, the purpose of this thesis is the following: generalize the fundamentals of multipoint multirate signal processing and apply these fundamentals to a data compression feasibility study based on the multiresolution wavelet decomposition with generalized sampling.

1.2 Thesis Layout

Chapter II will present the background of this thesis by providing a summary of the fundamentals of conventional multirate systems and wavelet theory. The basic multirate building blocks, the decimator and the expander, will be analyzed, and the conditions for perfect reconstruction will be presented. In addition, the fundamentals of the wavelet decomposition will be discussed, and the relationship between the wavelet decomposition and multirate systems will be examined.

In Chapter III, the theoretical foundations of multipoint multirate will be presented. The generalized multipoint building blocks, the block decimator and block expander, will be presented and the corresponding z-transforms will be derived. A method for generating perfect reconstruction multipoint multirate filter banks with vector lengths that vary from stage to stage will be presented. The application of the resulting perfect reconstruction multipoint multirate systems to the multiresolution wavelet decomposition will be studied.

In Chapter IV, a data compression feasibility study will be presented. It will be shown that signal energy can be redistributed between the levels of the multiresolution wavelet decomposition, and that this redistribution can theoretically increase the amount of data compression.

Chapter V will summarize the results of this thesis and outline recommendations for future research.

II. Background

2.1 Comb Filters

A comb filter is created from a prototype filter via the mapping $z \rightarrow z^M$. That is, given a prototype filter $Q(z)$, the z-transform of the comb filter for a given M is $Q(z^M)$. This implies a certain “pseudo-periodic” nature of the comb filter with period M .

Gianpaolo Evangelista [5] implemented a transform based on comb filters to separate the periodic trends in a signal from the period-to-period fluctuations. This was accomplished by matching the comb transformation M to the periodicity of the input signal.

It will be shown in chapter III that comb filters naturally arise in the study of multipoint multirate systems.

2.2 Conventional Multirate Fundamentals

2.2.1 Definitions. The two building blocks of multirate processing are the decimator and the expander [17, 2]. Both building blocks are linear, time-varying systems. The decimator is defined by the equation

$$y_D(n) = x(Mn)$$

where M is a positive integer, and the expander is defined by the equation

$$y_E(n) = \begin{cases} x(n/L) & , \text{ if } n \text{ is an integer multiple of } L \\ 0 & , \text{ else} \end{cases}$$

where L is a positive integer. Decimation by $M = 2$ retains every other point of a sequence, decimation by $M = 3$ retains every third point, etc. The value of M is the “decimation ratio”. Expansion by $L = 2$ places a zero between each point of

the original sequence, expansion by $L = 3$ places two zeros between each point of the original sequence, etc. The value of L is the “expansion ratio” [19, 2]. Figure 1 depicts examples of decimation and expansion on a sample sequence.

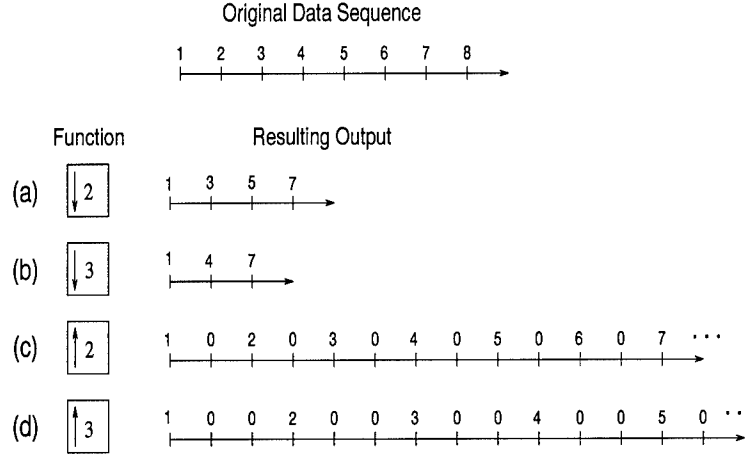


Figure 1. Examples of Decimation and Expansion. (a) Decimation by 2. (b) Decimation by 3. (c) Expansion by 2. (d) Expansion by 3.

If $y(n)$ is a decimated version of $x(n)$ with decimation ratio M , then the corresponding notation is given by $y(n) = (x(n)) \downarrow_M$. Similarly, if $y(n)$ is an expanded version of $x(n)$ with expansion ratio L , then the corresponding notation is given by $y(n) = (x(n)) \uparrow_L$. As shown in Figure 1, the block diagram of decimation by M is a down arrow along with the decimation ratio M , and the block diagram for expansion by L is an up arrow along with the expansion ratio L [17, 2].

2.2.2 z -Transforms of Building Blocks. The z -transforms of the basic building blocks of conventional multirate were summarized in the presentation of Crochiere and Rabiner [2]. The z -transform of an expanded sequence is defined by $Y_E(z) = X(z^L)$. Thus, the z -transform of $Y_E(z)$ is composed of compressed versions of the z -transform of the original sequence centered at every $2\pi/L$. The z -transform

of a decimated sequence is given by

$$Y_D(z) = \frac{1}{M} \sum_{k=0}^{M-1} X(z^{1/M} W^k), \quad W = \exp(-j2\pi/M)$$

The z-transform of $Y_D(z)$ is composed of stretched versions of the original z-transform centered at every 2π . Figure 2 provides an example of the Fourier Representation of expansion and decimation on a band limited signal. Figure 2c illustrates the phenomenon of “aliasing” (overlap of adjacent waveforms in the Fourier domain) caused by decimation. Moreover, when aliasing occurs, it is not in general possible to recover the original sequence from the decimated sequence [2].

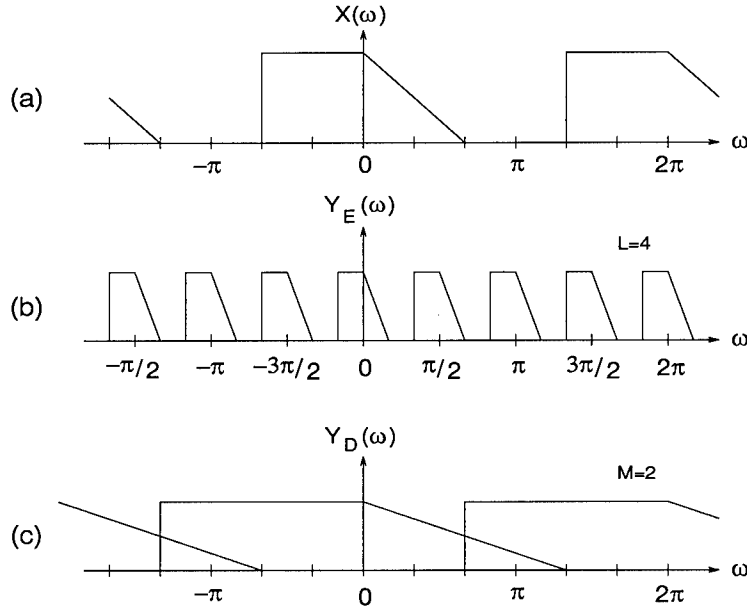


Figure 2. Fourier Representation of Decimation and Expansion. (a) Fourier representation of original sequence. (b) Fourier representation of sequence expanded by $L = 4$. (c) Fourier representation of sequence decimated by $M = 2$.

2.2.3 Manipulation of Building Blocks. After the Fourier representation of the decimator and expander were developed, Crochiere and Rabiner explored various ways to connect the building blocks [2]. Using the notation of section 2.2.1,

the following equations characterize the ways in which decimators can be combined together:

$$\alpha\{x(n)\} \downarrow_M = \{\alpha x(n)\} \downarrow_M, \quad \alpha \text{ any scalar}$$

$$\{x_1(n) + x_2(n)\} \downarrow_M = \{x_1(n)\} \downarrow_M + \{x_2(n)\} \downarrow_M$$

$$\{x_1(n) \times x_2(n)\} \downarrow_M = \{x_1(n)\} \downarrow_M \times \{x_2(n)\} \downarrow_M$$

Moreover, the same equations hold when the decimators are replaced with expanders.

Cascades of decimators and expanders can be exchanged only when the decimation ratio M and the expansion ratio L are relatively prime, i.e. $\gcd(M, L) = 1$. When this requirement on M and L holds, the following equation is valid:

$$\{\{x(n)\} \downarrow_M\} \uparrow_L = \{\{x(n)\} \uparrow_L\} \downarrow_M$$

The following two expressions provide the rules for the interchangeability of filters with the basic multirate building blocks:

$$\{X(z)G(z^M)\} \downarrow_M = \{X(z) \downarrow_M\} G(z)$$

$$\{X(z)G(z)\} \uparrow_L = \{X(z) \uparrow_L\} G(z^L)$$

These expressions are known as the Noble Identities [19]. It is important to note that the noble identities are only valid when $G(z)$ is comprised of integer powers of z . For example, the noble identities do not hold for $G(z) = z^{-1/2}$.

2.2.4 Polyphase Identities. The polyphase representation was originally developed by Maurice Bellanger et al [1] to describe the equivalence classes that result from the decomposition of a signal. In the mid 1980's, Martin Vetterli [22] and P.P Vaidyanathan [18] applied the polyphase representation to the study of multirate filter banks.

Consider the problem of breaking a filter $h(n)$ into its even and odd polyphase components. Let the z-transform of $h(n)$ be $H(z)$, that is, $H(z) = \sum_{n=-\infty}^{\infty} h(n)z^{-n}$. After separating $h(n)$ into the two subsequences $h(2n)$ and $h(2n+1)$, we obtain the following expression for $H(z)$:

$$\begin{aligned} H(z) &= \sum_{n=-\infty}^{\infty} h(2n)z^{-2n} + \sum_{n=-\infty}^{\infty} h(2n+1)z^{-(2n+1)} \\ &= \sum_{n=-\infty}^{\infty} h(2n)z^{-2n} + z^{-1} \sum_{n=-\infty}^{\infty} h(2n+1)z^{-2n} \end{aligned}$$

Let $E_0(z)$ and $E_1(z)$ represent the z-transforms of the two subsequences of $h(n)$, that is,

$$E_0(z) = \sum_{n=-\infty}^{\infty} h(2n)z^{-n}, \quad E_1(z) = \sum_{n=-\infty}^{\infty} h(2n+1)z^{-n}$$

Then, $H(z)$ can be written as

$$H(z) = E_0(z^2) + z^{-1}E_1(z^2)$$

These filters $E_0(z)$ and $E_1(z)$ are the even and odd polyphase components of the filter $H(z)$.

Figure 3 demonstrates how the polyphase components of a filter can be substituted into a multirate system. Figures 3a-3c demonstrate the replacement of $H(z)$ with $H(z) = E_0(z^2) + z^{-1}E_1(z^2)$. Applying the noble identities to the polyphase components results in the block diagram shown in figure 3d. This block diagram is also referred to as the polyphase representation of $H(z)$.

In general, the polyphase representation of a filter $H(z)$ for an arbitrary decimation ratio M is given by

$$H(z) = E_0(z^M) + z^{-1}E_1(z^M) + \cdots + z^{-(M-1)}E_{M-1}(z^M) = \sum_{i=0}^{M-1} z^{-i}E_i(z^M)$$

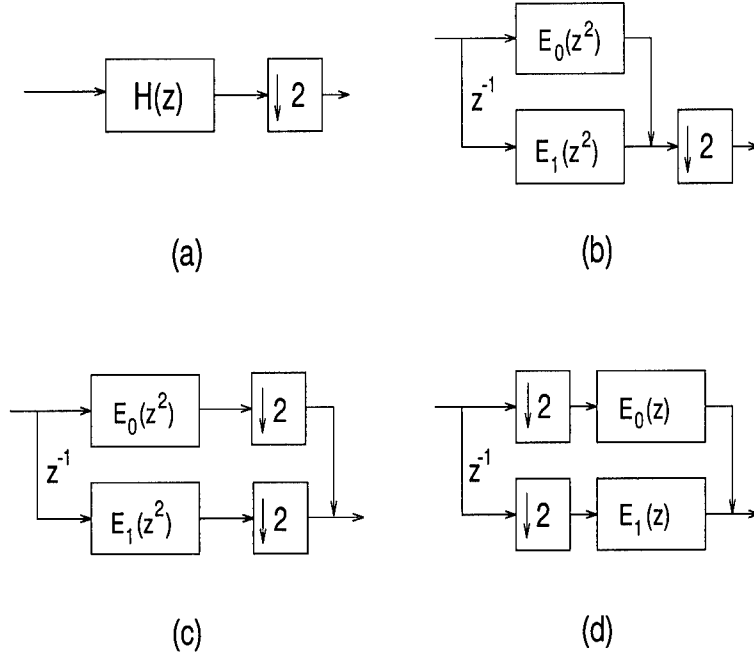


Figure 3. Polyphase Representation. (a) Original System. (b) Substitution of Polyphase Components for $H(z)$. (c) Splitting the Decimator. (d) Application of Noble Identities

$$\text{where } E_i(z) = \sum_{n=-\infty}^{\infty} h(Mn + i)z^{-n}.$$

The polyphase representation can also be derived for expanders instead of decimators. $H(z)$ is still written in terms of its polyphase components, except the second noble identity is used to pass the polyphase components back through the expanders.

2.3 Perfect Reconstruction Multirate Systems

A multirate filter bank is an M -channel system as shown in Figure 4. The set of filters $\{H_0(z) \cdots H_{M-1}(z)\}$ is called the “analysis bank” and the set of filters $\{F_0(z) \cdots F_{M-1}(z)\}$ is called the “synthesis bank” [20, 22, 17].

It is possible to choose the analysis and synthesis filters such that the output of the multirate system is a delayed (and possibly scaled) version of the input. Such

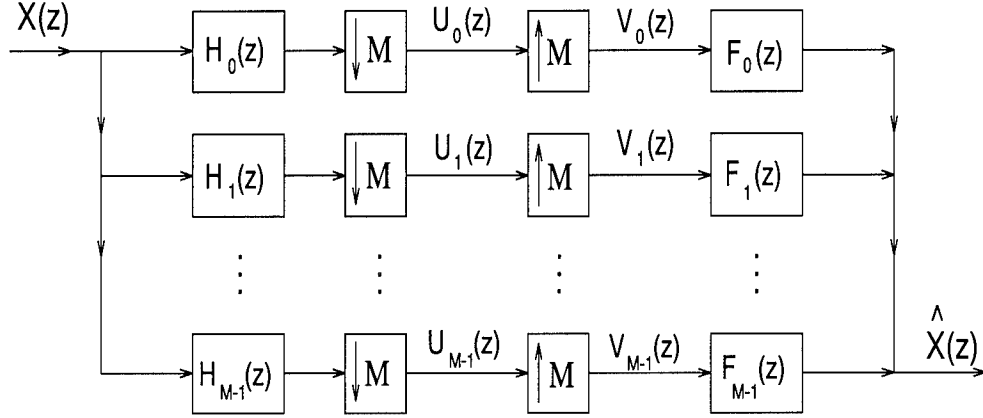


Figure 4. M Channel Multirate Filter Bank

a system is said to exhibit the “Perfect Reconstruction” property, or the “PR” property. This property was first studied by Smith and Barnwell [13] and Mintzer [11] for the two channel system, and later extended to the M channel system by Vetterli [22] and Vaidyanathan [18].

In an M channel multirate system, each of the filters $H_i(z)$ and $F_j(z)$ are written in terms of their M polyphase components $E_{ij}(z)$ and $R_{ij}(z)$. That is,

$$H_i(z) = \sum_{j=0}^{M-1} z^{-j} E_{i,j}(z^M)$$

$$F_j(z) = \sum_{i=0}^{M-1} z^{-(M-1-i)} R_{i,j}(z^M)$$

The polyphase components of the analysis filters can be placed into a polyphase matrix $E(z^M)$, where the i^{th} row of $E(z^M)$ is composed of the polyphase components of $H_i(z)$. In similar fashion, the polyphase components of the synthesis filters make

up the columns of the polyphase matrix $R(z^M)$. These polyphase matrices are:

$$E(z^M) = \begin{bmatrix} E_{0,0}(z^M) & E_{0,1}(z^M) & \cdots & E_{0,M-1}(z^M) \\ E_{1,0}(z^M) & E_{1,1}(z^M) & \cdots & E_{1,M-1}(z^M) \\ \vdots & \vdots & \ddots & \vdots \\ E_{M-1,0}(z^M) & E_{M-1,1}(z^M) & \cdots & E_{M-1,M-1}(z^M) \end{bmatrix}$$

and

$$R(z^M) = \begin{bmatrix} R_{0,0}(z^M) & R_{0,1}(z^M) & \cdots & R_{0,M-1}(z^M) \\ R_{1,0}(z^M) & R_{1,1}(z^M) & \cdots & R_{1,M-1}(z^M) \\ \vdots & \vdots & \ddots & \vdots \\ R_{M-1,0}(z^M) & R_{M-1,1}(z^M) & \cdots & R_{M-1,M-1}(z^M) \end{bmatrix}$$

After application of the noble identities to these polyphase matrices, the M channel multirate system shown in figure 4 can be redrawn as the M channel polyphase system shown in figure 5.

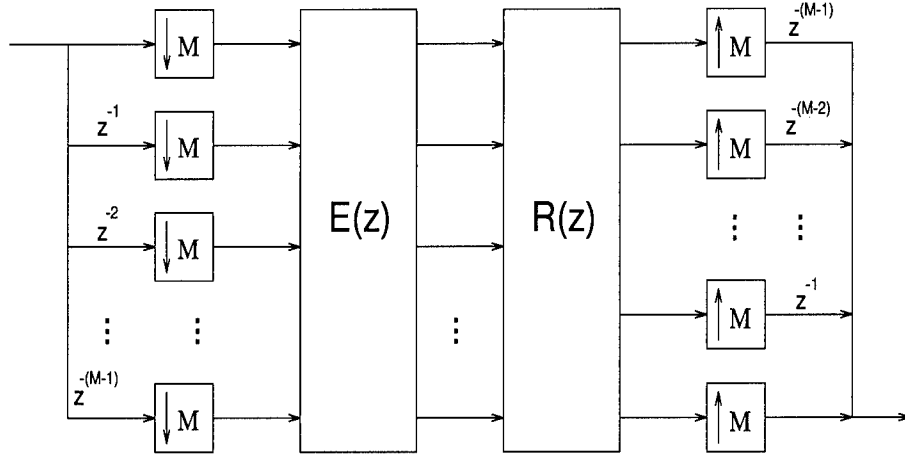


Figure 5. M Channel Multirate System with Polyphase Matrices

In this polyphase representation, the system exhibits perfect reconstruction [19] if and only if

$$P(z) = R(z)E(z) = cz^{-m_0} \begin{bmatrix} 0 & I_{M-r} \\ z^{-1}I_r & 0 \end{bmatrix}$$

where c is some scalar, m_0 is a nonnegative integer and $r \in \{0, 1, \dots, M-1\}$. Note that when $r = 0$, the equation becomes $P(z) = R(z)E(z) = cz^{-m_0}I_M$. In this case, $R(z)$ must be chosen such that $R(z) = cz^{-m_0}E^{-1}(z)$. In general, the inverse of $E(z)$ may not exist. If $E^{-1}(z)$ does exist, it may not be realizable with finite impulse response (FIR) filters, even if $E(z)$ is entirely composed of FIR filters. However, a special case arises when $E(z)$ is chosen to be “paraunitary”.

A matrix $E(z)$ is paraunitary if $E^{-1}(z) = \tilde{E}(z)$, where $\tilde{E}(z) \equiv E^H(z^{-1})$. That is, $\tilde{E}(z)$ is the complex conjugate transpose of $E(z)$ with z replaced by z^{-1} , and $\tilde{E}(z)E(z) = I$. Clearly, if $E(z)$ is paraunitary, then $R(z)$ can be chosen to equal $\tilde{E}(z)$ and the resulting $P(z)$ will equal the identity. For a maximally decimated filter bank, the perfect reconstruction property is equivalent to biorthogonality [4].

When $E(z)$ is paraunitary and $R(z) = \tilde{E}(z)$, then the resulting system will exhibit the PR property with the additional advantage that, if the analysis bank is composed of FIR filters, then the synthesis bank will also be composed of FIR filters. Thus, the special case of a paraunitary filter bank is very useful in the design of perfect reconstruction multirate systems [20, 22]. Moreover, if an orthonormal basis can be generated by using a tree structure (such as in the Discrete Wavelet Decomposition), then the basis can also be generated by a paraunitary tree [14]. Thus, a close relationship exists between paraunitariness and orthogonal decompositions.

2.4 Multiresolution Wavelet Decomposition and Multirate Signal Processing

2.4.1 Wavelet Decomposition Fundamentals. A recurring theme in the multiresolution wavelet decomposition is the successive projection of a function

into “smaller” orthogonal subspaces (see, for example, “Daubechies Ten Lectures on Wavelets”[3]).

Let $\{V_m\}_{m \in \mathcal{Z}}$ be a sequence of nested subspaces constructed in $L^2(\mathbb{R})$ such that $V_m \subset V_{m-1} \quad \forall m \in \mathcal{Z}$.

Let f be a function which exists in the subspace V_{m-1} . Let P_m be the projection operator which takes the function $f \in V_{m-1}$ into the nested subspace $V_m \subset V_{m-1}$. This projection operator eliminates the portion of f which is not in V_m , while it does not disturb the portion of f which lies in V_m . Clearly, successive application of the same projection operator does not effect the result, i.e., $(P_m)^k = P_m \quad \forall k \in \mathcal{Z}^+$.

Let $\{W_m\}_{m \in \mathcal{Z}}$ be another sequence of nested subspaces such that $W_m \subset V_{m-1} \quad \forall m \in \mathcal{Z}$. Further, let the span of $V_m \cup W_m$ equal V_{m-1} , and let V_m and W_m be orthogonal subspaces. Thus, $V_{m-1} = V_m \oplus W_m$ and $V_m \cap W_m = \phi$. Let $Q_m = \mathbf{I} - P_m$ (where \mathbf{I} is the identity operator) be the orthogonal projection operator which takes the function f into the nested subspace $W_m \subset V_{m-1}$. Thus, $P_m Q_m = Q_m P_m = \mathbf{0}$, where $\mathbf{0}$ is the zero operator.

Let the set of functions $\{\phi_{m,l}\}_{l \in \mathcal{Z}}$ be an orthonormal basis for V_m , and let the set of functions $\{\psi_{m,l}\}_{l \in \mathcal{Z}}$ be an orthonormal basis for W_m . Then, the projection of f into V_m can be expanded in terms of the basis functions for V_m , and the projection of f into W_m can be expanded in terms of the basis functions for W_m , resulting in the following equalities:

$$[P_m f](x) = \sum_l c_m(l) \phi_{m,l}(x)$$

$$[Q_m f](x) = \sum_l d_m(l) \psi_{m,l}(x)$$

To find a particular coefficient $c_m(l)$, one takes the inner product of $P_m f$ with the basis function $\phi_{m,l}$. The inner product of two arbitrary real valued functions f and g is defined by

$$\langle f, g \rangle = \int_{-\infty}^{\infty} f(t)g(t)dt$$

The inner product of $P_m f$ and $\phi_{m,l}$ is written as $\langle P_m f, \phi_{m,l} \rangle$. The inner product of any two basis functions is $\langle \phi_{m,l}, \phi_{m,k} \rangle = \delta_{k,l}$, since the basis functions are orthonormal. Therefore, a particular coefficient is found as follows:

$$\begin{aligned} \langle P_m f, \phi_{m,l} \rangle &= \langle \sum_k c_m(k) \phi_{m,k}, \phi_{m,l} \rangle \\ &= \sum_k c_m(k) \langle \phi_{m,k}, \phi_{m,l} \rangle \\ &= \sum_k c_m(k) \delta_{k,l} \\ &= c_m(l) \end{aligned}$$

We assume that the signal f exists entirely in the space V_{m-1} for some $m \in \mathcal{Z}$. That is, $P_{m-1}f = f$, and f can be completely represented as a linear combination of the basis functions for V_{m-1} . However, since $P_m + Q_m = \mathbf{I}$, we can write

$$P_{m-1}f = P_m f + Q_m f$$

Therefore, any particular decomposition coefficient in V_m can be written as

$$\begin{aligned} c_m(l) &= \langle P_m f, \phi_{m,l} \rangle \\ &= \langle (P_{m-1}f - Q_m f), \phi_{m,l} \rangle \\ &= \langle P_{m-1}f, \phi_{m,l} \rangle - \langle Q_m f, \phi_{m,l} \rangle \\ &= \langle P_{m-1}f, \phi_{m,l} \rangle \end{aligned}$$

This last equality holds because $Q_m f$ is in W_m , $\phi_{m,l}$ is a basis function for V_m , and V_m and W_m are orthogonal, so $\langle Q_m f, \phi_{m,l} \rangle = 0$.

If $P_{m-1}f$ is expanded in terms of the basis functions for V_{m-1} and the results substituted into the expression for $c_m(l)$, then

$$\begin{aligned} c_m(l) &= \langle P_m f, \phi_{m,l} \rangle \\ &= \langle (\sum_n c_{m-1}(n) \phi_{m-1,n}), \phi_{m,l} \rangle \\ &= \sum_n c_{m-1}(n) \langle \phi_{m-1,n}, \phi_{m,l} \rangle \end{aligned}$$

In similar fashion, it can be shown that

$$d_m(l) = \sum_n c_{m-1}(n) \langle \phi_{m-1,n}, \psi_{m,l} \rangle$$

For the case of discrete wavelet filters, the inner product of a basis function for V_{m-1} and a basis function for V_m can be written as an FIR filter, that is

$$\begin{aligned} \langle \phi_{m-1,n}, \phi_{m,l} \rangle &= h'(n - 2l) \\ \langle \phi_{m-1,n}, \psi_{m,l} \rangle &= g'(n - 2l) \end{aligned}$$

where the discrete wavelet filters h' and g' are independent of the decomposition level m . Thus, if the coefficients $c_{m-1}(n)$ of $f \in V_{m-1}$ are known, then the coefficients of the projection of f into V_m and W_m are

$$\begin{aligned} c_m(l) &= \sum_n c_{m-1}(n) h'(n - 2l) \\ d_m(l) &= \sum_n c_{m-1}(n) g'(n - 2l) \end{aligned}$$

where $c_m(l)$ are the coefficients of $P_m f \in V_m$ and $d_m(l)$ are the coefficients of $Q_m f \in W_m$.

Once the coefficients of the projection of f into V_m are known, the function can be further decomposed into the orthogonal subspaces of V_m , namely V_{m+1} and W_{m+1} , with the same formulas, since the discrete wavelet filters h' and g' are independent of the decomposition level m . This leads to a recursive decomposition routine, breaking f down into its projections into smaller orthogonal subspaces. This recursive algorithm is the heart of the modern multiresolution wavelet decomposition algorithm [12, 3, 10].

2.4.2 Relationship of the Wavelet Decomposition to Multirate Signal Processing. As shown in section 2.4.1, at decomposition level m the coefficients $c_m(n)$

can be written in terms of the coefficients at the next higher level as follows:

$$c_m(n) = \sum_k c_{m-1}(k) h'(k - 2n)$$

where $h'(n)$ is a filter which satisfies the wavelet decomposition requirements, i.e.,

$$h'(n - 2l) = \langle \phi_{m-1,n}, \phi_{m,l} \rangle$$

A new filter $h(n)$ can be created which is a “flipped” version of the filter $h'(n)$, that is, $h(n) = h'(-n)$. Substituting this filter $h(n)$ into the expression for the decomposition coefficients yields:

$$c_m(n) = \sum_k c_{m-1}(k) h(2n - k)$$

Note that, if $y(n) = (x(n)) \downarrow_2$, then $y(n) = x(2n)$. Thus, $c_m(n)$ can be written as

$$c_m(n) = \sum_k c_{m-1}(k) (h(n - k)) \downarrow_2$$

In section 2.2.3, we saw that $\alpha(x(n)) \downarrow_M = (\alpha x(n)) \downarrow_M$, where α is any scalar. Hence, $c_m(n)$ becomes

$$c_m(n) = \sum_k (c_{m-1}(k) h(n - k)) \downarrow_2$$

Also in section 2.2.3, we saw that $\{x_1(n) + x_2(n)\} \downarrow_M = \{x_1(n)\} \downarrow_M + \{x_2(n)\} \downarrow_M$. Hence, $c_m(n)$ can be written as

$$c_m(n) = \left(\sum_k c_{m-1}(k) h(n - k) \right) \downarrow_2$$

Also note that, for two signals $f(n)$ and $g(n)$, their discrete convolution is given by

$$f(n) * g(n) = \sum_k f(k)g(n - k)$$

Thus, the expression for the decomposition coefficients $c_m(n)$ can be simplified as

$$c_m(n) = (c_{m-1}(n) * h(n)) \downarrow_2$$

In similar fashion, the coefficients $c_{m-1}(n)$ projected into the space W_m are given by the expression

$$d_m(n) = (c_{m-1}(n) * g(n)) \downarrow_2$$

where $g(n) = g'(-n)$ and $g'(n)$ satisfies the wavelet decomposition requirement

$$g'(n - 2l) = \langle \phi_{m-1,n}, \psi_{m,l} \rangle$$

The filters $h(n)$ and $g(n)$ are traditionally chosen to be low pass and high pass filters, respectively. Thus, the coefficients $c_m(n)$ are referred to as the “low pass coefficients” or “coarse coefficients”, and the coefficients $d_m(n)$ are referred to as the “high pass coefficients” or “detail coefficients”[3].

With the above results, the decomposition of $c_{m-1}(n)$ into $c_m(n)$ and $d_m(n)$ can be viewed as a 2-channel multirate system, with the analysis bank comprised of the wavelet filters h and g . If h and g satisfy the wavelet decomposition requirements, then, in terms of multirate theory, the filters h and g form a perfect reconstruction set [19, 12]. Thus, the recursive wavelet decomposition algorithm can be viewed as a cascade of 2-channel multirate filters, as shown in figure 6. This figure demonstrates the realization of the wavelet decomposition as a perfect reconstruction multirate system.

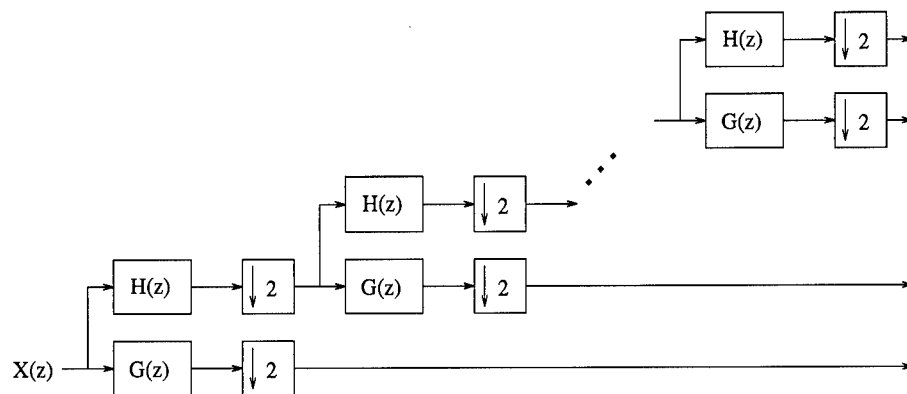


Figure 6. Multirate Implementation of the Multiresolution Wavelet Decomposition

III. Theoretical Foundations of Multipoint Multirate Signal Processing

3.1 Fundamentals of Multipoint Multirate Signal Processing

The fundamental building blocks of multipoint multirate are the multipoint decimator and the multipoint expander. These building blocks are modified from the conventional multirate building blocks (reference section 2.2.1) such that they operate on multiple points of data (data vectors) simultaneously. This is why multipoint multirate is also referred to as “vector sampling” [6].

For example, instead of retaining every other point as in conventional decimation by two, the multipoint decimator could retain the first two of every four points (or the first two points of each data vector of length four). This would correspond to multipoint decimation by (2,2). In general, multipoint decimation by (M, N) retains the first N points from every set of length MN . M is the decimation ratio, and N is the decimation vector length [6]. Multipoint expansion is defined in a similar manner. Multipoint expansion by (L, N) places $(L - 1)N$ zeros (or, equivalently, $L - 1$ zero-vectors each of length N) between each set of N data points [6]. See Figure 7 for examples of multipoint decimation and expansion. Note that multipoint decimation or expansion by $(M, 1)$ is equivalent to conventional decimation or expansion by M .

3.1.1 Definition of the Multipoint Decimator. The equation of the multipoint decimator can be written as $y(n) = x(\lfloor n/N \rfloor MN + n \text{MOD} N)$, where the floor function of k , denoted $\lfloor k \rfloor$, is the greatest integer $\leq k$. This expression for the multipoint decimator is comprised of two fundamental pieces. The first, $\lfloor n/N \rfloor MN$, accounts for the periodicity in a decimated signal. The original sequence is blocked into vectors of length MN , and then these vectors are mapped into $y(n)$ with period N . The second term, $n \text{MOD} N$, maps the first N elements of every length MN input vector into the output $y(n)$. Thus, as n increases, the first term indexes the length

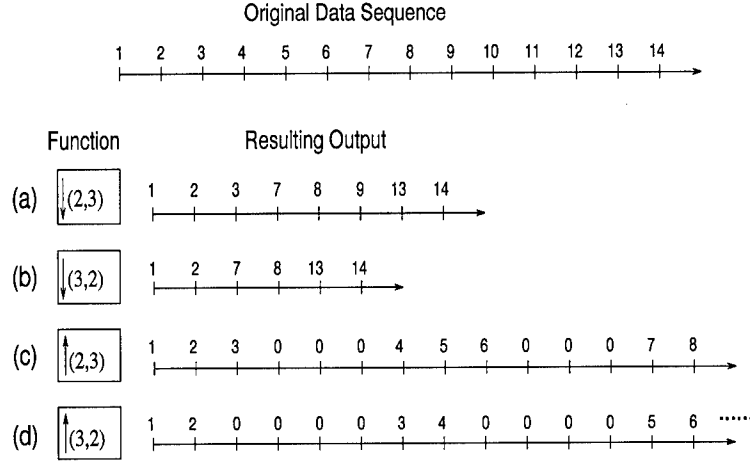


Figure 7. Examples of Multipoint Decimation and Expansion. (a) Decimation by (2,3). (b) Decimation by (3,2). (c) Expansion by (2,3). (d) Expansion by (3,2).

MN data vectors, and the second term steps through the first N points of data in each vector.

Note that, when $N = 1$, this equation reduces to $y(n) = x(Mn)$. This is the equation describing the single point decimator [2] which was discussed in section 2.2.

3.1.2 z -transform Analysis of the Multipoint Decimator. In the z -transform domain, the equivalent circuit of multipoint decimation by (M, N) is shown in figure 8. This equivalent circuit blocks the original sequence into vectors of length MN , but only retains the first N points of every vector. This is multipoint decimation by (M, N) .

The building blocks in the equivalent circuit of figure 8 are all conventional decimators and expanders which were discussed in section 2.2. As such, the z -transform of the multipoint decimator, which will be denoted as $(X(z)) \downarrow_{M,N}$, is:

$$X(z) \downarrow_{M,N} = \frac{1}{MN} \sum_{k=0}^{MN-1} \left(\sum_{l=0}^{N-1} z^{l\frac{1-M}{M}} W_{MN}^{lk} \right) X(z^{\frac{1}{M}} W_{MN}^k)$$

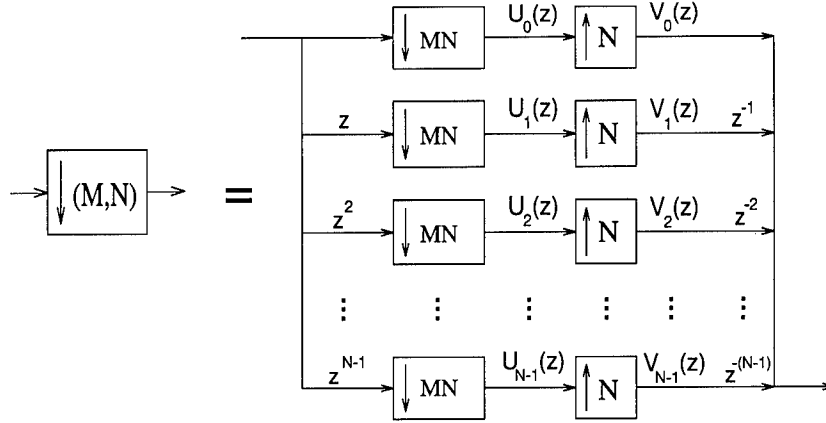


Figure 8. Equivalent Circuit for Multipoint Decimator

where $W_{MN}^k = \exp(-j2\pi k/(MN))$. This equation was derived as follows. Let $U_l(z)$ be the output of the decimator in the l^{th} channel of the equivalent circuit. Then,

$$\begin{aligned} U_l(z) &= (X(z)z^l) \downarrow_{MN} \\ &= \frac{1}{MN} \sum_{k=0}^{MN-1} X(z^{\frac{1}{MN}} W_{MN}^k) z^{\frac{l}{MN}} W_{MN}^{lk} \end{aligned}$$

Let $V_l(z)$ be the output of the expander in the l^{th} channel of the equivalent circuit. Then,

$$\begin{aligned} V_l(z) &= (U_l(z)) \uparrow_N \\ &= U_l(z^N) \\ &= \frac{1}{MN} \sum_{k=0}^{MN-1} X(z^{\frac{N}{MN}} W_{MN}^k) z^{\frac{lN}{MN}} W_{MN}^{lk} \\ &= \frac{1}{MN} \sum_{k=0}^{MN-1} X(z^{\frac{1}{M}} W_{MN}^k) z^{\frac{l}{M}} W_{MN}^{lk} \end{aligned}$$

Now, the output of the equivalent circuit, $\hat{X}(z)$, is

$$\hat{X}(z) = \sum_{l=0}^{N-1} z^{-l} V_l(z)$$

$$\begin{aligned}
&= \sum_{l=0}^{N-1} z^{-l} \left(\frac{1}{MN} \sum_{k=0}^{MN-1} X(z^{\frac{1}{M}} W_{MN}^k) z^{\frac{l}{M}} W_{MN}^{lk} \right) \\
&= \frac{1}{MN} \sum_{k=0}^{MN-1} \sum_{l=0}^{N-1} X(z^{\frac{1}{M}} W_{MN}^k) z^{-l} z^{\frac{l}{M}} W_{MN}^{lk} \\
&= \frac{1}{MN} \sum_{k=0}^{MN-1} \left(\sum_{l=0}^{N-1} z^{l(\frac{1-M}{M})} W_{MN}^{lk} \right) X(z^{\frac{1}{M}} W_{MN}^k)
\end{aligned}$$

In the last equation, the term inside the large parentheses is independent of the input $X(z)$; it is only a function of M, N , and k . This term will be called the “Decimation Scaling Function”, and it will be denoted AD_{MN}^k . Hence, the output of the multipoint decimator is given by

$$X(z) \Big|_{M,N} = \frac{1}{MN} \sum_{k=0}^{MN-1} AD_{MN}^k X(z^{\frac{1}{M}} W_{MN}^k)$$

This equation demonstrates that multipoint decimation with a decimation ratio of M and a vector length of N creates $MN - 1$ alias terms, whereas conventional decimation with a decimation ratio of M creates only $M - 1$ alias terms.

3.1.3 Polyphase Analysis of the Multipoint Decimator. As stated above, the multipoint decimator blocks the data into vectors of length MN , but only retains the first N points of each vector. As shown in figure 8, this blocking is performed by a bank of N conventional decimators, each with decimation ratio MN .

The input to the decimator in the first channel of the equivalent circuit is $x(n)$, so the output of this decimator is given by $y(n) = x(MNn)$. As shown in section 2.2.1, the MN polyphase representation of any signal $x(n)$ is

$$X(z) = \sum_{k=0}^{MN-1} E_k(z^{MN}) z^{-k}$$

where $E_k(z) = \sum_n x(MNn + k)z^{-n} = \sum_n e_k(n)z^{-n}$. Thus, the output of the first decimator in the equivalent circuit is $y(n) = e_0(n)$, where $e_0(n)$ is the first of the MN polyphase components of the input signal $x(n)$.

In similar fashion, the input to the decimator in the k^{th} channel of the equivalent circuit is $z^k X(z)$. This can be written in terms of its polyphase components $E'(z)$ (where the prime demonstrates that these are not the polyphase components of $X(z)$ from above) as follows:

$$z^k X(z) = \sum_{m=0}^{MN-1} E'_m(z^{MN})z^{-m}$$

However, by substituting the polyphase representation for $X(z)$ into $z^{-k}X(z)$, the following equivalent expression is derived:

$$\begin{aligned} z^k X(z) &= z^k \left(\sum_{l=0}^{MN-1} E_l(z^{MN})z^{-l} \right) \\ &= \sum_{l=0}^{MN-1} E_l(z^{MN})z^{-(l-k)} \end{aligned}$$

By making the change of variable $m = l - k$, we have

$$\begin{aligned} z^k X(z) &= \sum_{m=-k}^{MN-1-k} E_{m+k}(z^{MN})z^{-m} \\ &= \sum_{m=0}^{MN-1-k} E_{m+k}(z^{MN})z^{-m} + \sum_{m=MN-k}^{MN-1} E_{m+k+MN}(z^{MN})z^{-m-MN} \end{aligned}$$

But the polyphase representation of $z^k X(z)$ in terms of its own polyphase components is

$$z^k X(z) = \sum_{m=0}^{MN-1} E'_m(z^{MN})z^{-m}$$

By equating this expression for $z^k X(z)$ with the above expression for $z^k X(z)$, we find that $E'_0(z) = E_k(z)$. Decimation by MN in each channel of the equivalent circuit retains only the first polyphase component of the input signal, so the output

of the decimator in the k^{th} channel of the equivalent circuit will be the k^{th} polyphase component of the input signal $X(z)$.

These signals are subsequently expanded by N and multiplied by z^{-k} , so the final output $Y_k(z)$ of each channel in the equivalent circuit is $Y_k(z) = z^{-k}E_k(z^N)$. Forming the summation of these $Y_k(z)$ yields the polyphase decimation expression for the output of a multipoint decimator, which is equivalent to the decimation relation derived in section 3.1.2. This alternate representation with decimation ratio M and vector length N is given by:

$$\hat{X}(z) = \sum_{k=0}^{N-1} z^{-k} E_k(z^N)$$

In this polyphase expression for the multipoint decimator, the Decimation Scaling Function has served to eliminate the higher order polyphase components in each channel of the equivalent circuit. The resulting expression is the first N of the MN polyphase components of the input signal $x(n)$, each component expanded by N and shifted an appropriate amount. In general, the original signal $x(n)$ is not recoverable because the highest $(M - 1)N$ polyphase components have been discarded.

3.1.4 Definition of the Multipoint Expander. The equation of the multipoint expander can be written as

$$y(n) = \begin{cases} x(\lfloor n/(NM) \rfloor N + n \text{MOD}(MN)) & , \text{ if } n \text{MOD}(MN) < N \\ 0 & , \text{ else} \end{cases}$$

This expression also has two fundamental pieces. The first, $\lfloor n/(NM) \rfloor N$, controls the periodicity of the multipoint expansion. The input signal is blocked into vectors of length N , and this term indexes those vectors. The second term, $n \text{MOD}(MN)$, indexes the points of data inside the vector. When this term is less

than N , it maps the N points of the length N data vector into the output $y(n)$. Then, for $N \leq n \text{MOD}(MN) \leq MN - 1$, a set of $(M - 1)N$ zeros are mapped into the output. Thus, as n increases, consecutive blocks of length N of the input signal are mapped to the output with $M - 1$ zero-vectors of length N inserted between the data vectors.

Note that, when the expansion vector length $N = 1$, this equation reduces to

$$y(n) = \begin{cases} x(n/M) & , \text{ if } n \text{ is divisible by } M \\ 0 & , \text{ else} \end{cases}$$

This is the equation describing the conventional expander [2], which was discussed in section 2.2.

3.1.5 z-transform Analysis of the Multipoint Expander. In the z -transform domain, the equivalent circuit of the multipoint expander with expansion ratio M and vector length N is shown in figure 9. This equivalent circuit blocks the original sequence into vectors of length N and then inserts $M - 1$ zero-vectors of length N between the data vectors.

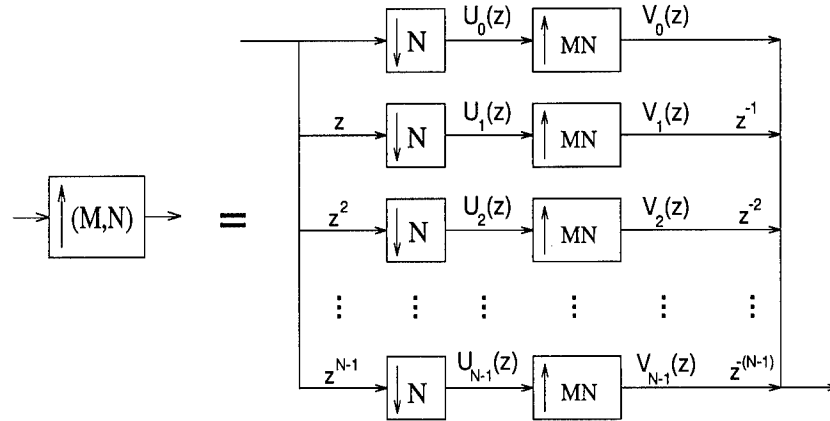


Figure 9. Equivalent Circuit for Multipoint Expander

The building blocks in the equivalent circuit of figure 9 are all conventional decimators and expanders which were discussed in section 2.2. As such, the z-transform of the multipoint expander, which will be denoted as $(X(z)) \uparrow_{M,N}$, is:

$$X(z) \uparrow_{M,N} = \frac{1}{N} \sum_{k=0}^{N-1} \left(\sum_{l=0}^{N-1} z^{l(M-1)} W_N^{lk} \right) X(z^M W_N^k)$$

This equation was derived as follows:

Let $U_l(z)$ be the output of the decimator in the l^{th} channel of the equivalent circuit. Then,

$$\begin{aligned} U_l(z) &= (X(z)z^l) \downarrow_N \\ &= \frac{1}{N} \sum_{k=0}^{N-1} X(z^{\frac{1}{N}} W_N^k) z^{\frac{l}{N}} W_N^{lk} \end{aligned}$$

Let $V_l(z)$ be the output of the expander in the l^{th} channel of the equivalent circuit. Then,

$$\begin{aligned} V_l(z) &= (U_l(z)) \uparrow_{MN} \\ &= U_l(z^{MN}) \\ &= \frac{1}{N} \sum_{k=0}^{N-1} X(z^{\frac{MN}{N}} W_N^k) z^{\frac{lMN}{N}} W_N^{lk} \\ &= \frac{1}{N} \sum_{k=0}^{N-1} X(z^M W_N^k) z^{lM} W_N^{lk} \end{aligned}$$

Now, the output of the equivalent circuit, $\hat{X}(z)$, is

$$\begin{aligned} \hat{X}(z) &= \sum_{l=0}^{N-1} z^{-l} V_l(z) \\ &= \sum_{l=0}^{N-1} z^{-l} \left(\frac{1}{N} \sum_{k=0}^{N-1} X(z^M W_N^k) z^{lM} W_N^{lk} \right) \end{aligned}$$

$$\begin{aligned}
&= \frac{1}{N} \sum_{k=0}^{N-1} \sum_{l=0}^{N-1} \left(z^{-l} z^{lM} W_N^{lk} X(z^M W_N^k) \right) \\
&= \frac{1}{N} \sum_{k=0}^{N-1} \left(\sum_{l=0}^{N-1} z^{l(M-1)} W_N^{lk} \right) X(z^M W_N^k)
\end{aligned}$$

The term inside the large parentheses is again independent of the input $X(z)$, and is only a function of M, N , and k . This term will be called the “Expansion Scaling Function”, and it will be denoted AE_{MN}^k . It can be used to simplify the equation of the multipoint expander to

$$X(z) \Big|_{M,N} = \frac{1}{N} \sum_{k=0}^{N-1} AE_{MN}^k X(z^M W_N^k)$$

In the next section, it will be shown that this scaling function is a byproduct of the blocking nature of the multipoint expander. It is important to note that there is no aliasing in the multipoint expander, and the original signal is completely recoverable from the expanded signal.

3.1.6 Polyphase Analysis of the Multipoint Expander. As stated above, the multipoint decimator blocks the data into vectors of length N , and then places $M - 1$ zero-vectors of length N between the blocks of data. As shown in figure 9, this blocking is performed by a bank of N conventional decimators, each with decimation ratio N .

This data-blocking bank of decimators is similar to the blocking nature of the decimator, except the data are blocked into vectors of length N and all the blocks are retained. Thus, with minor modification to the derivation of section 3.1.1, the output of the decimator in the k^{th} channel of the equivalent circuit will be the k^{th} polyphase component of the input signal $X(z)$.

These polyphase components are subsequently expanded by MN and multiplied by z^{-k} , so the final output $Y_k(z)$ of each channel in the equivalent circuit is

$Y_k(z) = z^{-k} E_k(z^{MN})$. Forming the summation of these $Y_k(z)$ yields the polyphase expansion expression for the output of a multipoint expander, which is equivalent to the expansion relation derived in section 3.1.4. This alternate representation with expansion ratio M and vector length N is given by:

$$\hat{X}(z) = \sum_{k=0}^{N-1} z^{-k} E_k(z^{MN})$$

In this polyphase expression for the multipoint decimator, the Expansion Scaling Function has served to eliminate the higher order polyphase components in each channel of the equivalent circuit. The resulting expression is comprised of all N of the N polyphase components for the input signal $x(n)$. The components have been expanded by MN and shifted to comprise the complete expanded signal. The original signal is completely recoverable by reblocking the expanded signal into vectors of length MN and then only retaining the first N points of each block. As discussed in section 3.1.2, this inverse operation is multipoint decimation.

3.1.7 Interconnections of Building Blocks. This section provides proofs for the basic interconnection properties of the multipoint decimator and expander. These interconnection properties are depicted (for the multipoint decimator) in figures 10, 11, and 12. The first two properties demonstrate that the multipoint building blocks are linear operators.

3.1.7.1 Scaling a Decimated Sequence by a Constant α . A sequence can be multiplied by a scalar prior to or after multipoint decimation; the results are identical. See figure 10.

$$\begin{aligned} Y(z) &= \alpha [X(z)] \downarrow_{M,N} \\ &= \alpha \left[\frac{1}{MN} \sum_{k=0}^{MN-1} \left(\sum_{l=0}^{N-1} z^{l(\frac{1-M}{M})} W_{MN}^{lk} \right) X(z^{\frac{1}{M}} W_{MN}^k) \right] \end{aligned}$$

$$\begin{aligned}
&= \frac{1}{MN} \sum_{k=0}^{MN-1} \left(\sum_{l=0}^{N-1} z^{l(\frac{1-M}{M})} W_{MN}^{lk} \right) [\alpha X(z^{\frac{1}{M}} W_{MN}^k)] \\
&= [\alpha X(z)] \downarrow_{M,N}
\end{aligned}$$

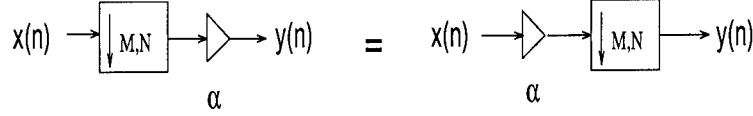


Figure 10. Scaling a Decimated Sequence by a Scalar

3.1.7.2 Adding Two Decimated Sequences. Multipoint decimation can be performed on the sum of two sequences, or the decimation can be performed prior to the summation. In either case, the results are identical. See figure 11.

$$\begin{aligned}
Y(z) &= [X_1(z) + X_2(z)] \downarrow_{M,N} \\
&= \frac{1}{MN} \sum_{k=0}^{MN-1} \left(\sum_{l=0}^{N-1} z^{l(\frac{1-M}{M})} W_{MN}^{lk} \right) [X_1(z^{\frac{1}{M}} W_{MN}^k) + X_2(z^{\frac{1}{M}} W_{MN}^k)] \\
&= \frac{1}{MN} \sum_{k=0}^{MN-1} \left(\sum_{l=0}^{N-1} z^{l(\frac{1-M}{M})} W_{MN}^{lk} \right) X_1(z^{\frac{1}{M}} W_{MN}^k) \\
&\quad + \frac{1}{MN} \sum_{k=0}^{MN-1} \left(\sum_{l=0}^{N-1} z^{l(\frac{1-M}{M})} W_{MN}^{lk} \right) X_2(z^{\frac{1}{M}} W_{MN}^k) \\
&= [X_1(z)] \downarrow_{M,N} + [X_2(z)] \downarrow_{M,N}
\end{aligned}$$

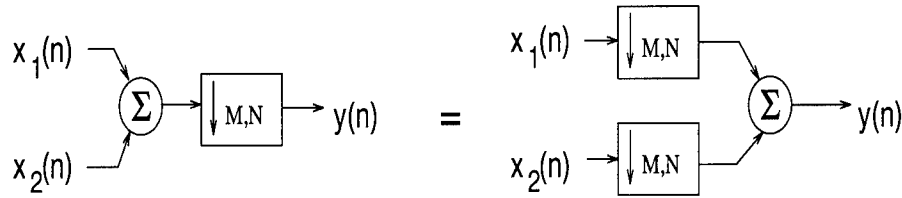


Figure 11. Adding Two Decimated Sequences

3.1.7.3 Multiplying Two Decimated Sequences. Two sequences may be multiplied point by point prior to or after multipoint decimation. The results are

the same either way. To prove this, the following relationship is required:

If $u(n) = x(n) \times d(n)$, then $U(e^{j\omega}) = X(e^{j\omega}) * D(e^{j\omega})$, where $*$ denotes convolution.

Therefore, if

$$y(n) = [x(n) \times d(n)] \downarrow_{M,N}$$

then, in the Fourier domain,

$$\begin{aligned} Y(e^{j\omega}) &= [X(e^{j\omega}) * D(e^{j\omega})] \downarrow_{M,N} \\ &= \frac{1}{MN} \sum_{k=0}^{MN-1} \left(\sum_{l=0}^{N-1} e^{j\omega l (\frac{1-M}{M})} W_{MN}^{lk} \right) [X(e^{j\omega \frac{1}{M}} W_{MN}^k) * D(e^{j\omega \frac{1}{M}} W_{MN}^k)] \end{aligned}$$

and, since convolution is linear in each variable (i.e. bilinear),

$$\begin{aligned} Y(e^{j\omega}) &= \frac{1}{MN} \sum_{k=0}^{MN-1} \left(\sum_{l=0}^{N-1} e^{j\omega l (\frac{1-M}{M})} W_{MN}^{lk} \right) X(e^{j\omega \frac{1}{M}} W_{MN}^k) \\ &\quad * \frac{1}{MN} \sum_{k=0}^{MN-1} \left(\sum_{l=0}^{N-1} e^{j\omega l (\frac{1-M}{M})} W_{MN}^{lk} \right) D(e^{j\omega \frac{1}{M}} W_{MN}^k) \\ &= [X(e^{j\omega})] \downarrow_{M,N} * [D(e^{j\omega})] \downarrow_{M,N} \end{aligned}$$

Thus, in time,

$$y(n) = [x(n)] \downarrow_{M,N} \times [d(n)] \downarrow_{M,N}$$

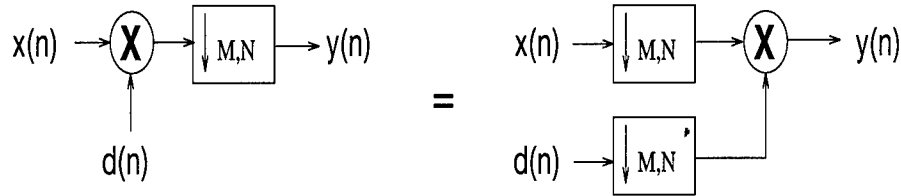


Figure 12. Multiplying Two Decimated Sequences

These three equalities all hold true when multipoint expansion is substituted for multipoint decimation.

3.1.8 *Multipoint Noble Identities.* The Noble Identities for multipoint decimators and expanders are depicted in figures 13a and 13b. The proofs for these identities are presented below:

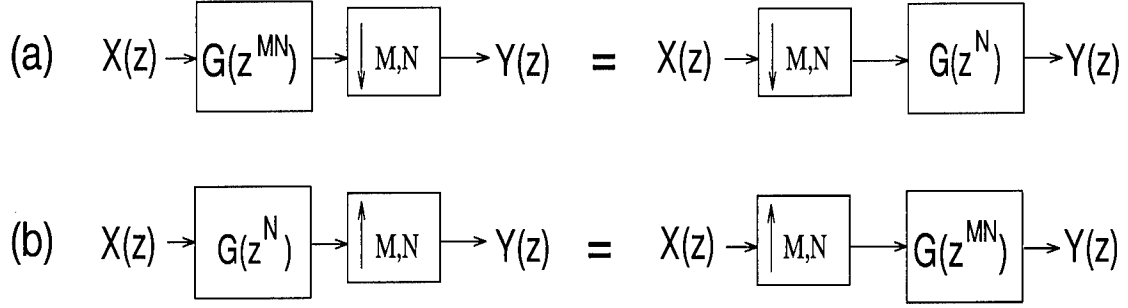


Figure 13. Multipoint Noble Identities. (a) First Noble Identity. (b) Second Noble Identity

3.1.8.1 *The First (Decimation) Noble Identity (Figure 13a).*

$$\begin{aligned}
 Y(z) &= [X(z)G(z^{MN})] \downarrow_{M,N} \\
 &= \frac{1}{MN} \sum_{k=0}^{MN-1} \left(\sum_{l=0}^{N-1} z^{l(\frac{1-M}{M})} W_{MN}^{lk} \right) X(z^{\frac{1}{M}} W_{MN}^k) G(z^N W_{MN}^{MNk}) \\
 &= \frac{1}{MN} \sum_{k=0}^{MN-1} \left(\sum_{l=0}^{N-1} z^{l(\frac{1-M}{M})} W_{MN}^{lk} \right) X(z^{\frac{1}{M}} W_{MN}^k) G(z^N) \\
 &= G(z^N) [X(z)] \downarrow_{M,N}
 \end{aligned}$$

3.1.8.2 *The Second (Expansion) Noble Identity (Figure 13b).*

$$\begin{aligned}
 Y(z) &= [X(z)G(z^N)] \uparrow_{M,N} \\
 &= \frac{1}{N} \sum_{k=0}^{N-1} \left(\sum_{l=0}^{N-1} z^{l(N-1)} W_N^{lk} \right) X(z^M W_N^k) G(z^{MN} W_N^{Nk}) \\
 &= \frac{1}{N} \sum_{k=0}^{N-1} \left(\sum_{l=0}^{N-1} z^{l(N-1)} W_N^{lk} \right) X(z^M W_N^k) G(z^{MN}) \\
 &= G(z^{MN}) [X(z)] \uparrow_{M,N}
 \end{aligned}$$

3.1.9 Multipoint Polyphase Representation. In order to develop the multipoint polyphase identities for a filter $H(z)$, the filter must be decomposed into its MN conventional polyphase components. The resulting polyphase equation for multipoint decimation with decimation ratio M and vector length N is given by

$$H(z) = \sum_{k=0}^{MN-1} E_k(z^{MN})z^{-k}$$

where

$$E_k(z) = \sum_{n=-\infty}^{\infty} h(MNn + k)z^{-n}$$

For an M channel multipoint multirate system with analysis filters $\{H_0(z), H_1(z), \dots, H_{MN-1}(z)\}$, the polyphase representation for $H_l(z)$ is

$$H_l(z) = \sum_{k=0}^{MN-1} E_{l,k}(z^{MN})z^{-k}$$

These polyphase components can be arranged into a matrix $E(z^{MN})$, where the l^{th} row of $E(z^{MN})$ is comprised of the polyphase components of $H_l(z)$. Thus, the analysis bank can be represented by the following polyphase matrix:

$$E(z^{MN}) = \begin{bmatrix} E_{0,0}(z^{MN}) & E_{0,1}(z^{MN}) & \cdots & E_{0,MN-1}(z^{MN}) \\ E_{1,0}(z^{MN}) & E_{1,1}(z^{MN}) & \cdots & E_{1,MN-1}(z^{MN}) \\ \vdots & \vdots & & \vdots \\ E_{M-1,0}(z^{MN}) & E_{M-1,1}(z^{MN}) & \cdots & E_{M-1,MN-1}(z^{MN}) \end{bmatrix}$$

This matrix can be passed through the multipoint decimators by applying the first multipoint noble identity presented in section 3.1.8. The resulting polyphase representation of the multipoint analysis bank is shown in figure 14.

Since there are MN polyphase components of each filter $H_l(z)$ and there are M analysis filters (an M channel system), the polyphase matrix $E(z)$ is $M \times MN$. The decimation vector length N generates a redundancy in this representation (in

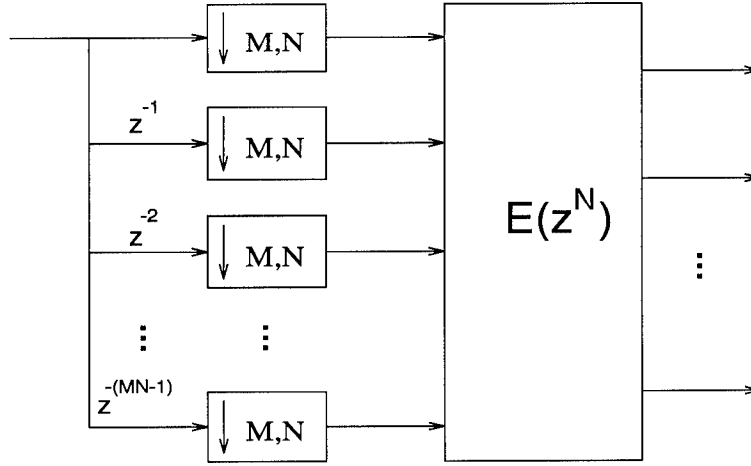


Figure 14. Multipoint Polyphase Representation

a conventional M channel multirate system, the polyphase matrix is $M \times M$). This redundancy will cause comb filters (reference section 2.1) to arise when perfect reconstruction multirate filter banks are designed.

Recently, Suter and Xia [23] presented an alternate representation of the multipoint polyphase matrix. They called this representation “vector polyphase”. In the vector polyphase representation, there are only M channels in the resulting polyphase system, but the resulting vector polyphase matrix, $\mathbf{E}(\mathbf{z})$, has dimension $MN \times MN$. Thus, the redundancy is still present and built directly into the vector polyphase matrix.

3.1.10 Conditions for Perfect Reconstruction in Multipoint Multirate Systems. The output of a multipoint multirate system is typically multiple combinations of the polyphase components of the input signal $x(n)$. These components are scaled and shifted in such a way that the original signal is not, in general, recoverable from this output. This is due to the fact that multipoint decimators create aliasing, and multipoint building blocks are time varying operators. However, it is possible to control the analysis and synthesis filters which make up the multipoint multirate system such that the output $\hat{X}(z)$ of the system is a scaled and delayed

version of the input $X(z)$ to the system. That is, $\hat{X}(z) = cz^{-m_0}X(z)$ for some scalar c and some integer m_0 . When this is true, the multipoint multirate system exhibits the perfect reconstruction property.

3.1.10.1 Vector Polyphase Requirement for Perfect Reconstruction.

Given the vector polyphase representation $\mathbf{E}(\mathbf{z})$ of an analysis bank and the vector polyphase representation $\mathbf{R}(\mathbf{z})$ of a synthesis bank, the multipoint multirate system exhibits perfect reconstruction if and only if [23]

$$\mathbf{P}(\mathbf{z}) = \mathbf{R}(\mathbf{z})\mathbf{E}(\mathbf{z}) = c z^{-m_0} \begin{bmatrix} 0 & I_{M-r} \\ z^{-1}I_r & 0 \end{bmatrix} \otimes I_N$$

where c is any scalar, m_0 is a nonnegative integer, $r \in \{0, 1, \dots, M-1\}$, and \otimes denotes the tensor product. If the vector polyphase representation $\mathbf{E}(\mathbf{z})$ of a multipoint analysis bank is made to be paraunitary, and $\mathbf{R}(\mathbf{z})$ chosen such that $\mathbf{R}(\mathbf{z}) = \tilde{\mathbf{E}}(\mathbf{z})$, then the multipoint multirate system will be a perfect reconstruction system [23]. These properties can all be tied to the multipoint polyphase representation developed in section 3.1.

3.1.11 Multipoint Polyphase Requirements for Perfect Reconstruction. Figure 15 shows the polyphase representation of a multipoint multirate system with decimation ratio M and vector length N . Note that the polyphase representation has MN channels due to the redundancy of this notation. The matrix $P(z^N)$ shown in figure 15 is the multipoint system polyphase matrix $P(z) = R(z)E(z)$, where $E(z)$ and $R(z)$ are the polyphase representations of the multipoint analysis bank

and synthesis bank, respectively. Thus,

$$E(z^N) = \begin{bmatrix} E_{0,0}(z^N) & E_{0,1}(z^N) & \cdots & E_{0,MN-1}(z^N) \\ E_{1,0}(z^N) & E_{1,1}(z^N) & \cdots & E_{1,MN-1}(z^N) \\ \vdots & \vdots & \ddots & \vdots \\ E_{MN-1,0}(z^N) & E_{MN-1,1}(z^N) & \cdots & E_{MN-1,MN-1}(z^N) \end{bmatrix}$$

$$R(z^N) = \begin{bmatrix} R_{0,0}(z^N) & R_{0,1}(z^N) & \cdots & R_{0,M-1}(z^N) \\ R_{1,0}(z^N) & R_{1,1}(z^N) & \cdots & R_{1,M-1}(z^N) \\ \vdots & \vdots & \ddots & \vdots \\ R_{MN-1,0}(z^N) & R_{MN-1,1}(z^N) & \cdots & R_{MN-1,M-1}(z^N) \end{bmatrix}$$

$$P(z^N) = \begin{bmatrix} P_{0,0}(z^N) & P_{0,1}(z^N) & \cdots & P_{0,MN-1}(z^N) \\ P_{1,0}(z^N) & P_{1,1}(z^N) & \cdots & P_{1,MN-1}(z^N) \\ \vdots & \vdots & \ddots & \vdots \\ P_{MN-1,0}(z^N) & P_{MN-1,1}(z^N) & \cdots & P_{MN-1,MN-1}(z^N) \end{bmatrix}$$

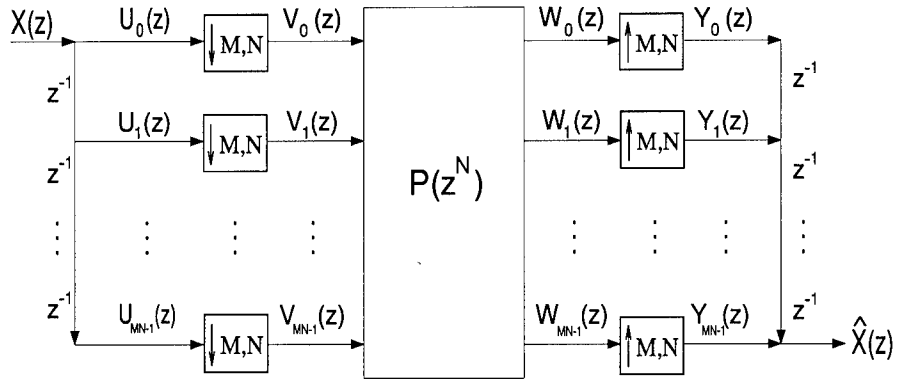


Figure 15. Multipoint System with Polyphase Matrix $P(z)$

In order to find the conditions required for perfect reconstruction in the multipoint multirate system shown in figure 15, it is necessary to find the transfer function of the entire system. That is, given an input signal $X(z)$, what is the output $\hat{X}(z)$?

The expressions for the output of multipoint decimators and expander derived in section 3.1 make this analysis possible.

Given the input signal $X(z)$, the input to the multipoint decimator in each channel of the polyphase system is given by $U_k(z) = X(z)z^{-k}$, where $k \in \{0, 1, \dots, MN - 1\}$ is the number of the channel. The output of each decimator is $V_k(z)$, where

$$\begin{aligned} V_k(z) &= (U_k(z)) \downarrow_{M,N} \\ &= \sum_{l=0}^{MN-1} z^{-l} E'_l(z^{MN}) \end{aligned}$$

where the $E'_l(z)$ are the MN polyphase components of $U_k(z)$.

$U_k(z)$ can be written in terms of the polyphase components of $X(z)$ as follows:

$$\begin{aligned} X(z) &= \sum_{l=0}^{MN-1} z^{-l} E_l(z^{MN}) \\ U_k(z) &= X(z)z^{-k} \\ &= z^{-k} \sum_{l=0}^{MN-1} z^{-l} E_l(z^{MN}) \\ &= \sum_{l=0}^{MN-1} z^{-(l+k)} E_l(z^{MN}) \end{aligned}$$

Making the change of variables $\gamma = l + k$, we find that

$$\begin{aligned} U_k(z) &= \sum_{\gamma=k}^{MN-1+k} z^{-\gamma} E_{\gamma+k}(z^{MN}) \\ &= \sum_{\gamma=k}^{MN-1} z^{-\gamma} E_{\gamma+k}(z^{MN}) + \sum_{\gamma=MN}^{MN-1+k} z^{-\gamma} E_{\gamma+k}(z^{MN}) \\ &= \sum_{\gamma=k}^{MN-1} z^{-\gamma} E_{\gamma+k}(z^{MN}) + \sum_{\gamma=0}^{k-1} z^{-\gamma-MN} E_{\gamma+MN-k}(z^{MN}) \\ &= \sum_{\gamma=k}^{MN-1} z^{-\gamma} E_{\gamma+k}(z^{MN}) + z^{-MN} \sum_{\gamma=0}^{k-1} z^{-\gamma} E_{\gamma+MN-k}(z^{MN}) \end{aligned}$$

But the expression for $U_k(z)$ in terms of its own polyphase components $E'_l(z)$ is given by

$$U_k(z) = \sum_{l=0}^{MN-1} z^{-l} E'_l(z^{MN})$$

By equating this expression for $U_k(z)$ and the previous expression for $U_k(z)$, we find that

$$E'_l(z^{MN}) = \begin{cases} E_{l-k}(z^{MN}) & \text{for } k \leq l \leq MN-1 \\ z^{-MN} E_{l-k+MN}(z^{MN}) & \text{for } 0 \leq l \leq k-1 \end{cases}$$

and the final expression for $U_k(z)$ is

$$U_k(z) = \sum_{l=0}^{k-1} z^{-MN} z^{-l} E_{l+MN-k}(z^{MN}) + \sum_{l=k}^{MN-1} z^{-l} E_{l-k}(z^{MN})$$

The output of the decimator in channel k is given by

$$\begin{aligned} V_k(z) &= (U_k(z)) \downarrow_{M,N} \\ &= \sum_{n=0}^{N-1} E_{k_n}(z^N) z^{-n} \end{aligned}$$

where the $E_{k_n}(z)$ are the MN polyphase components (indexed by n) of the signal $U_k(z)$.

However, we know that

$$E_{k_n}(z) = \begin{cases} z^{-1} E_{n+MN-k}(z) & \text{for } 0 \leq n \leq k-1 \\ E_{n-k}(z) & \text{for } k \leq n \leq MN-1 \end{cases}$$

and k is limited to the range $0 \leq k \leq N-1$. Therefore, the expression for the output of the decimator in each channel is given by

$$V_k(z) = \sum_{n=0}^{k-1} z^{-N} E_{n+MN-k}(z^N) z^{-n} + \sum_{n=k}^{N-1} E_{n-k}(z^N) z^{-n}$$

Now, the polyphase system matrix $P(z^N)$ is applied to the output of the decimators. In each channel, this is accomplished by taking the inner product of the k^{th} row of $P(z^N)$ with the column vector whose entries are the outputs of the decimators. This result is given by

$$\begin{aligned} W_k(z) &= z^{-N} \sum_{n=0}^{l-1} z^{-n} \left(\sum_{l=0}^{MN-1} P_{kl}(z^N) E_{n+MN-l}(z^N) \right) \\ &\quad + \sum_{n=l}^{N-1} z^{-n} \left(\sum_{l=0}^{MN-1} P_{kl}(z^N) E_{n-l}(z^N) \right) \\ &= \sum_{n=0}^{N-1} z^{-n} \left(\sum_{l=0}^{MN-1} P_{kl}(z^N) \mathcal{E}(n, l, z^N) \right) \end{aligned}$$

where

$$\mathcal{E}(n, l, z) = \begin{cases} E_{n-l}(z) & l \leq n \leq N-1 \\ z^{-1} E_{n+MN-l}(z) & 0 \leq n \leq l-1 \end{cases}$$

By close observation of this expression for $W_k(z)$, we find that the expression inside the large parentheses is completely composed of powers of z^N . Thus, the n^{th} polyphase component of $W_k(z)$ is given by

$$\sum_{l=0}^{MN-1} P_{kl}(z^N) \mathcal{E}(n, l, z^N)$$

The output of the multipoint expander is given by

$$Y_k(z) = (W_k(z)) \uparrow_{M,N} = \sum_{m=0}^{N-1} z^{-m} F_{km}(z^{MN})$$

where $F_{km}(z)$ are the $0 \leq m \leq N-1$ polyphase components of $W_k(z)$.

Therefore, the complete expression for the output of each expander is

$$Y_k(z) = \sum_{m=0}^{N-1} z^{-m} \left(\sum_{l=0}^{MN-1} P_{kl}(z^{MN}) \mathcal{E}(m, l, z^{MN}) \right)$$

and, multiplying each $Y_k(z)$ by $z^{-(M-1-k)}$ and summing over k , the expression for the output of the multipoint multirate system is given by

$$\hat{X}(z) = \sum_{k=0}^{MN-1} z^{-(MN-1-k)} \left(\sum_{m=0}^{N-1} z^{-m} \left(\sum_{l=0}^{MN-1} P_{kl}(z^{MN}) \mathcal{E}(m, l, z^{MN}) \right) \right)$$

where

$$\mathcal{E}(m, l, z) = \begin{cases} E_{m-l}(z) & l \leq m \leq N-1 \\ z^{-1} E_{m+MN-l}(z) & 0 \leq m \leq l-1 \end{cases}$$

are the NM polyphase components of the original input signal $X(z)$.

Now that we have an expression for the output of the multipoint polyphase system, it can be analyzed to find the conditions needed for perfect reconstruction. The polyphase components of $X(z)$ are all present in the above equation, but they are weighted by various entries of $P(z)$ and summed three different times. In order for the system to exhibit perfect reconstruction, the output must include each polyphase component of $X(z)$, and they must be weighted by cz^{-m_0+k} , where c is a scaler, m_0 is an integer, and k is the number of the polyphase component. If $P = I$, then this condition will hold.

Unfortunately, it is not possible for P to equal the identity. P is the product of the $MN \times M$ matrix R and the $M \times MN$ matrix E . Therefore, the rank of P can be no greater than M , and P cannot be row-equivalent to the identity matrix. However, P does not have to equal the identity.

Define the matrix $\delta_{N_{ij}}$ to be the singular matrix of zeros with the single entry at position i, j equal to one. Let $P(z) = I_M \otimes \delta_{N_{00}}$. Thus, $P(z)$ is a matrix of zeros, with M equally spaced values of one on the main diagonal. A multipoint multirate system with such a $P(z)$ will exhibit the perfect reconstruction property. The proof is given below.

Let $\hat{X}_\alpha(z)$ be a polyphase component of the system output $\hat{X}(z)$. To select this component out of the expression for $\hat{X}(z)$, the values of m and k must be selected

such that $\mathcal{E}(m, k, z)$ is a function of only $E_\alpha(z)$. Also, we know that $P_{i,j} = 1$ if $i = j$ and i is a multiple of N , and $P_{i,j} = 0$ otherwise. With this information, the expression for $\hat{X}_\alpha(z)$ becomes

$$\begin{aligned} \hat{X}_\alpha(z) = & \sum_{k=0}^{MN-1-\alpha} z^{-(MN-1-k)} \left(z^{-(\alpha+k)} P_{kk}(z^{MN}) E_\alpha(z^{MN}) \right) \dots \\ & \sum_{k=MN-\alpha}^{MN-1} z^{-(MN-1-k)} \left(z^{-(\alpha+k-MN)} P_{kk}(z^{MN}) z^{-MN} E_\alpha(z^{MN}) \right) \end{aligned}$$

This equation reduces to

$$\hat{X}_\alpha(z) = M E_\alpha(z^{MN}) z^{-(MN-1+\alpha)}$$

Thus, when $P(z) = I_M \otimes \delta_{\mathbf{N}00}$, each of the MN polyphase component of the input $X(z)$ appears at the output, they are appropriately expanded and delayed, and the system satisfies the perfect reconstruction property.

In general, sufficient conditions for perfect reconstruction in the multipoint multirate system are

$$P(z) = cz^{-m_0} \begin{bmatrix} \mathbf{0} & I_{M-r} \\ z^{-1}I_r & \mathbf{0} \end{bmatrix} \otimes \delta_{\mathbf{N}ij}$$

where c is any scalar, m_0 is an integer, and $0 \leq r \leq M-1$. For a proof of these general conditions, see Appendix B.

If the polyphase matrices $E(z)$ and $R(z)$ are chosen such that $R(z) = \tilde{E}(z)$, then the perfect reconstruction requirement demands that the columns of $E(z)$ be orthogonal. However, since the rank of $E(z)$ is at most M , only M of the columns can be linearly independent. Thus, $E(z)$ must be chosen such that only M of its columns are non-zero. Of course, these M non-zero columns must be orthogonal to

each other. When $E(z)$ and $R(z)$ are chosen in this manner, the resulting $P(z)$ is sufficient for perfect reconstruction.

This requirement on $E(z)$ can be related back to the polyphase components of the original filter bank. Recall that

$$E(z) = \begin{bmatrix} E_{0,0}(z) & E_{0,1}(z) & \cdots & E_{0,MN-1}(z) \\ E_{1,0}(z) & E_{1,1}(z) & \cdots & E_{1,MN-1}(z) \\ \vdots & \vdots & & \vdots \\ E_{M-1,0}(z) & E_{M-1,1}(z) & \cdots & E_{M-1,MN-1}(z) \end{bmatrix}$$

The k^{th} row of $E(z)$ is composed of the MN polyphase components of the analysis filter $H_k(z)$. However, if $E(z)$ satisfies the perfect reconstruction condition, then only M of these MN entries are non-zero. That is, the filter $H_k(z)$ only has polyphase components $E_{k,l}(z)$ where l is a multiple of M . Thus,

$$\begin{aligned} H_k(z) &= \sum_{l=0}^{MN-1} E_l(z^{MN}) z^{-l} \\ &= \sum_{n=0}^{M-1} E_n(z^M) z^{-nN} \end{aligned}$$

because the polyphase components $E_l(z)$ are zero for l not a multiple of N .

If we let some prototype filter $H'_k(z)$ be defined by

$$H'_k(z) = \sum_{n=0}^{M-1} E_n(z^M) z^{-n}$$

it becomes clear that $H_k(z) = (H'_k(z)) \uparrow_N$. That is, $H_k(z)$ is created from the prototype filter $H'_k(z)$ by conventional expansion by N . $H_k(z)$ is a comb filter (reference section 2.1).

This analysis demonstrates how comb filters naturally arise in multipoint multirate systems. If the sufficient conditions for perfect reconstruction are to hold, the

filters which make up the analysis and synthesis banks must be comb filters created from some set of prototype filters. Also, these prototype filter must form a conventional paraunitary set to ensure that the columns of the multipoint polyphase matrix $E(z)$ are orthogonal. This provides a quick method for generating perfect reconstruction multipoint systems for various vector lengths from a set of conventional perfect reconstruction filters.

3.1.12 Design of Perfect Reconstruction Filter Banks using the Vector Polyphase Notation. The design of perfect reconstruction filter banks can also be accomplished from an analysis of the vector polyphase notation [23]. The same results will be found to hold: the resulting filters for vector length N are comb filters generated by conventional expansion by N .

Given the properties of perfect reconstruction (PR) multipoint multirate systems presented in section 3.1.10, the goal is to design an analysis filter bank and a synthesis filter bank such that the multirate system satisfies the PR property. This can be accomplished by choosing the analysis filters such that the vector polyphase matrix $\mathbf{E}(\mathbf{z})$ is paraunitary, then choosing the synthesis filters such that $\mathbf{R}(\mathbf{z}) = \tilde{\mathbf{E}}(\mathbf{z})$ [23]. The problem lies in designing an analysis bank such that the resulting vector polyphase matrix $\mathbf{E}(\mathbf{z})$ is paraunitary.

Let T_N be a linear transformation. Given a set of prototype filters $\{H'_0(z), H'_1(z), \dots, H'_{M-1}(z)\}$ which satisfy the PR property in a conventional multirate system, does there exist a set of filters $\{T_N[H'_0(z)], T_N[H'_1(z)], \dots, T_N[H'_{M-1}(z)]\}$ which satisfy the PR property for a multipoint multirate system with vector length N ?

In the traditional multiresolution wavelet decomposition, decimation by two is performed at each stage. The vector representation of a filter $H(z)$ with decimation

ratio $M = 2$ and vector length N is given by Xia and Suter [23] to be

$$\mathbf{H}(\mathbf{z}) = \begin{bmatrix} H_0(z) & z^{-1}H_{N-1}(z) & z^{-1}H_{N-2}(z) & \cdots & z^{-1}H_1(z) \\ H_1(z) & H_0(z) & z^{-1}H_{N-1}(z) & \cdots & z^{-1}H_2(z) \\ H_2(z) & H_1(z) & H_0(z) & \cdots & z^{-1}H_3(z) \\ \vdots & \vdots & \vdots & \ddots & \vdots \\ H_{N-1}(z) & H_{N-2}(z) & H_{N-3}(z) & \cdots & H_0(z) \end{bmatrix}$$

In general, bold face denotes the vector representation of a filter, and normal font denotes the scalar form of a filter.

A close analysis of the derivation of this matrix yields that the entries of $\mathbf{H}(\mathbf{z})$ are actually the N conventional polyphase components of the filter $H(z)$. That is, if

$$H(z) = \sum_{k=0}^{N-1} E_k(z^N)z^{-k}$$

then the vector matrix representation of $H(z)$ is

$$\mathbf{H}(\mathbf{z}) = \begin{bmatrix} E_0(z) & z^{-1}E_{N-1}(z) & z^{-1}E_{N-2}(z) & \cdots & z^{-1}E_1(z) \\ E_1(z) & E_0(z) & z^{-1}E_{N-1}(z) & \cdots & z^{-1}E_2(z) \\ E_2(z) & E_1(z) & E_0(z) & \cdots & z^{-1}E_3(z) \\ \vdots & \vdots & \vdots & \ddots & \vdots \\ E_{N-1}(z) & E_{N-2}(z) & E_{N-3}(z) & \cdots & E_0(z) \end{bmatrix}$$

Each of the entries of $\mathbf{H}(\mathbf{z})$ can be broken into its two conventional polyphase components. That is, we can replace each $E_i(z)$ with its polyphase representation

$$E_i(z) = E_{i,0}(z^2) + z^{-1}E_{i,1}(z^2)$$

After substituting these polyphase components for every entry of $\mathbf{H}(\mathbf{z})$, then $\mathbf{H}(\mathbf{z})$ can then be split into two submatrices. The first is composed entirely of even

powers of z , and the second composed of odd powers of z . This expression for $\mathbf{H}(z)$ is:

$$\mathbf{H}(z) = \mathbf{E}_E(z^2) + z^{-1}\mathbf{E}_O(z^2)$$

where

$$\mathbf{E}_E(z^2) = \begin{bmatrix} E_{0,0}(z^2) & z^{-2}E_{N-1,1}(z^2) & \cdots & z^{-2}E_{1,1}(z^2) \\ E_{1,0}(z^2) & E_{0,0}(z^2) & \cdots & z^{-2}E_{2,1}(z^2) \\ \vdots & \vdots & \ddots & \vdots \\ E_{N-1,0}(z^2) & E_{N-2,0}(z^2) & \cdots & E_{0,0}(z^2) \end{bmatrix}$$

and

$$\mathbf{E}_O(z^2) = \begin{bmatrix} E_{0,1}(z^2) & E_{N-1,0}(z^2) & \cdots & E_{1,0}(z^2) \\ E_{1,1}(z^2) & E_{0,1}(z^2) & \cdots & E_{2,0}(z^2) \\ \vdots & \vdots & \ddots & \vdots \\ E_{N-1,1}(z^2) & E_{N-2,1}(z^2) & \cdots & E_{0,1}(z^2) \end{bmatrix}$$

These matrices $\mathbf{E}_E(z^2)$ and $\mathbf{E}_O(z^2)$ are the vector polyphase components of the matrix $\mathbf{H}(z)$. The elements of these vector polyphase matrices are actually the $2N$ conventional polyphase components of the filter $H(z)$.

The goal of this analysis is to relate the elements of the vector polyphase matrices to the polyphase components of a base filter, $H'(z)$. Assume that the base filter $H'(z)$ is part of a perfect reconstruction set for a conventional multirate filter bank with decimation ratio $M = 2$. Assume that the filter $H(z)$ (from which the vector polyphase matrices above were derived) is part of the analysis bank for a multipoint multirate system with decimation ratio $M = 2$ and vector length N .

Now, assume that $H(z) = T_N \{H'(z)\}$, where the linear transformation, T_N , is conventional expansion by N . The resulting filter $H(z) = (H'(z)) \uparrow_N = H'(z^N)$ is a “comb filter” [5]

The conventional polyphase representation of $H'(z)$ with $M = 2$ is

$$H'(z) = E'_E(z^2) + z^{-1}E'_O(z^2)$$

Thus, the filter $H(z)$ can be written in terms of the conventional polyphase components of $H'(z)$ as follows:

$$\begin{aligned} H(z) &= H'(z^N) \\ &= E'_E(z^{2N}) + z^{-N}E'_O(z^{2N}) \end{aligned}$$

However, representing $H(z)$ in terms of its own N conventional polyphase components yields

$$\begin{aligned} H(z) &= \sum_{k=0}^{N-1} E_k(z^N)z^{-k} \\ &= E_0(z^N) + z^{-1}E_1(z^N) + \cdots + z^{-(N-1)}E_{N-1}(z^N) \end{aligned}$$

By equating terms in this expression for $H(z)$ and the previous expression for $H(z)$, we find that the conventional polyphase components are related by

$$E_0(z^N) = E'_E(z^{2N}) + z^{-N}E'_O(z^{2N})$$

and

$$E_i(z^N) = 0$$

for $i \neq 0$.

The vector representation $\mathbf{H}(\mathbf{z})$ of the filter $H(z)$ can now be written in terms of the conventional polyphase components of the prototype filter $H'(z)$ as follows:

$$\mathbf{H}(\mathbf{z}) = \begin{bmatrix} E'_E(z^2) + z^{-1}E'_O(z^2) & \mathbf{0} \\ & \ddots \\ \mathbf{0} & E'_E(z^2) + z^{-1}E'_O(z^2) \end{bmatrix}$$

By splitting this matrix into its even and odd vector polyphase matrices $\mathbf{E}_E(\mathbf{z})$ and $\mathbf{E}_O(\mathbf{z})$, an expression for $\mathbf{H}(\mathbf{z})$ can be derived in terms of the conventional polyphase components of the prototype filter $H'(z)$.

$$\mathbf{H}(\mathbf{z}) = \mathbf{E}_E(\mathbf{z}^2) + z^{-1}\mathbf{E}_O(\mathbf{z}^2)$$

where

$$\mathbf{E}_E(\mathbf{z}^2) = \begin{bmatrix} E'_E(z^2) & \mathbf{0} \\ & \ddots \\ \mathbf{0} & E'_E(z^2) \end{bmatrix}$$

and

$$\mathbf{E}_O(\mathbf{z}^2) = \begin{bmatrix} E'_O(z^2) & \mathbf{0} \\ & \ddots \\ \mathbf{0} & E'_O(z^2) \end{bmatrix}$$

The elements in these two vector polyphase matrices are the conventional polyphase components of the prototype filter $H'(z)$.

The same analysis can be used to derive the vector polyphase representation of a second filter $G(z)$. That is, it is assumed that $G(z) = G'(z^N)$, that $G'(z)$ is part of a conventional perfect reconstruction multirate system, and that the conventional polyphase representation of $G'(z)$ with $M = 2$ is given by

$$G'(z) = F'_E(z^2) + z^{-1}F'_O(z^2)$$

With these assumptions, the vector polyphase matrix $\mathbf{E}(\mathbf{z})$ for the complete two channel multipoint multirate system with decimation ratio $M = 2$ and vector length N is given by

$$\mathbf{E}(\mathbf{z}) = \begin{bmatrix} \mathbf{E}_E(\mathbf{z}) & \mathbf{E}_O(\mathbf{z}) \\ \mathbf{F}_E(\mathbf{z}) & \mathbf{F}_O(\mathbf{z}) \end{bmatrix}$$

$$= \begin{bmatrix} E'_E(z) & \mathbf{0} & E'_O(z) & \mathbf{0} \\ & \ddots & & \ddots \\ \mathbf{0} & E'_E(z) & \mathbf{0} & E'_O(z) \\ F'_E(z) & \mathbf{0} & F'_O(z) & \mathbf{0} \\ & \ddots & & \ddots \\ \mathbf{0} & F'_E(z) & \mathbf{0} & F'_O(z) \end{bmatrix}$$

If the conventional polyphase matrix $E(z)$ of the set of filters $H'(z)$ and $G'(z)$ is paraunitary, then the vector polyphase matrix $\mathbf{E}(\mathbf{z})$ formed from $H(z)$ and $G(z)$ will also be paraunitary, and the resulting multipoint multirate system with decimation ratio $M = 2$ and vector length N will exhibit perfect reconstruction.

This result reiterates the result of section 3.1.11, in that a multipoint perfect reconstruction set can be constructed from comb filters. This provides a simple and quick algorithm for generating perfect reconstruction multipoint multirate filter banks. Given a set of conventional perfect reconstruction filters (which are readily available in the literature [17, 19, 2, 22]), a new set of perfect reconstruction filters can be easily formed for a multipoint multirate system for any vector decimation length. Thus, the wavelet decomposition can be generalized to include varying vector lengths at each level. With the above methods for generating perfect reconstruction filter banks, only one set of prototype filters is necessary. The multipoint filters for each vector length are generated as comb filters from the prototype filters, and

the resulting generalized wavelet decomposition satisfies the perfect reconstruction property.

3.2 Wavelet Decomposition with Multipoint Multirate Systems

The traditional binary tree structured wavelet decomposition using a multirate filter bank was shown in figure 16 and discussed in section 2.4.2. The filters $H(z)$ and $G(z)$ which make up the analysis bank are typically a low pass filter and high pass filter respectively, and together they form a perfect reconstruction set (paraunitary pair).

By applying the algorithm developed in section 3.1.12, a new perfect reconstruction pair $H_{N_k}(z)$ and $G_{N_k}(z)$ can be generated for any vector length N_k from the original filters $H(z)$ and $G(z)$. Thus, the conventional decimators and expanders in the wavelet tree can be replaced with multipoint decimators and expanders. If the filters at each level of the tree are replaced with the appropriately chosen $H_{N_k}(z)$ and $G_{N_k}(z)$, then the entire system will still exhibit the perfect reconstruction property. The resulting multipoint wavelet decomposition tree with generic vector lengths is shown in Figure 16.

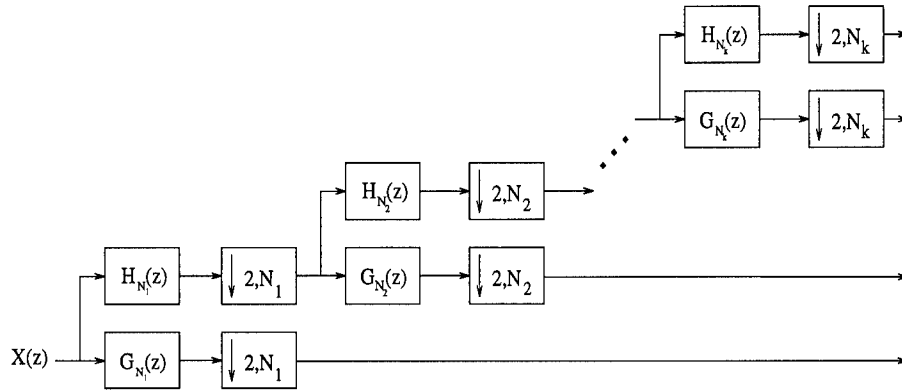


Figure 16. Multipoint Wavelet Decomposition Tree with Generic Decimation Vector Lengths

The advantage of such a system is that the decimation vector length can be varied at each level, thus redistributing the energy of the original signal throughout the decomposition tree. The choice of vector lengths may be made such that the energy distribution of the decomposed signal is optimal in some sense. Thus, by processing a signal with new decomposition algorithm, a higher rate of data compression may be achieved.

IV. A Data Compression Feasibility Study

4.1 Introduction

The goal is to achieve superior data compression over the traditional multiresolution wavelet decomposition by employing multipoint multirate in the binary decomposition tree. This approach will permit the decimation vector length N to be varied at each level of the decomposition. Section 4.2 will explore methods of increasing the data compression by redistributing the energy in the high frequency subbands [15].

4.2 Energy Redistribution Between Levels of the Multiresolution Analysis.

At each level of the wavelet decomposition, the coefficients are decimated by a factor of two. However, only the coarse coefficients are further decomposed. If the energy of the signal happens to be concentrated at a coarse decomposition level, fewer coefficients/bits will be needed to represent that signal than if the signal energy is concentrated at the more detailed levels which underwent less decimation. Thus, improved data compression should be achievable if the energy of the signal can be forced down to the coarser decomposition levels.

Figures 17 and 18 show a paraunitary prototype filter set and the related comb filters which can be used in a multipoint multirate perfect reconstruction system. The Daubechies filter D_8 was chosen as the prototype because it has compact support and a relatively narrow transition band. This "sharpness" of the filter allows for a decomposition based on the spectral content of a signal, without the increased processing time of a larger filter.

Each of the filters shown in figures 17 and 18 can be part of a perfect reconstruction set if the decimation vector lengths are chosen appropriately.

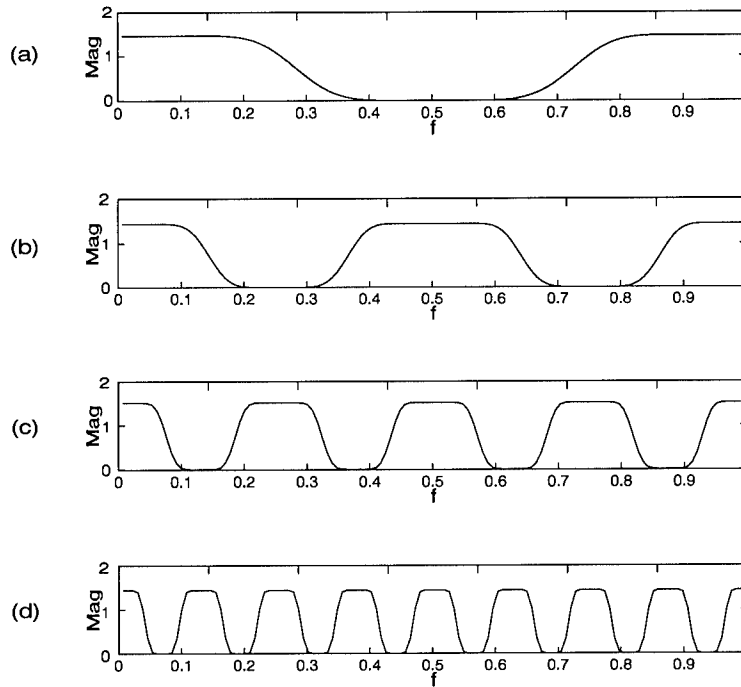


Figure 17. Daubechies Low Pass Filter $H(z)$ for Various Vector Lengths. (a) Prototype Filter. (b) Vector Length of 2. (c) Vector Length of 4. (d) Vector Length of 8

At each stage of the decomposition, the signal is divided into a low frequency and high frequency subband via application of H and G , respectively. The low frequency band is then decomposed again, as shown in figure 16. In the traditional multiresolution wavelet decomposition, only conventional multirate building blocks are used, so the only choice of filters are the standard low pass H and high pass G (shown in figures 17a and 18a). However, when the wavelet decomposition is generalized to allow multipoint decimation with varying vector lengths at each level of the decomposition (as shown in figure 16), any of the filters from figure 17 can be used. The choice of decimation vector length N (or , equivalently, the choice of expansion ratio applied to the prototype filters H and G) can be made at each level to maximize the amount of signal energy passed into the low frequency subband.

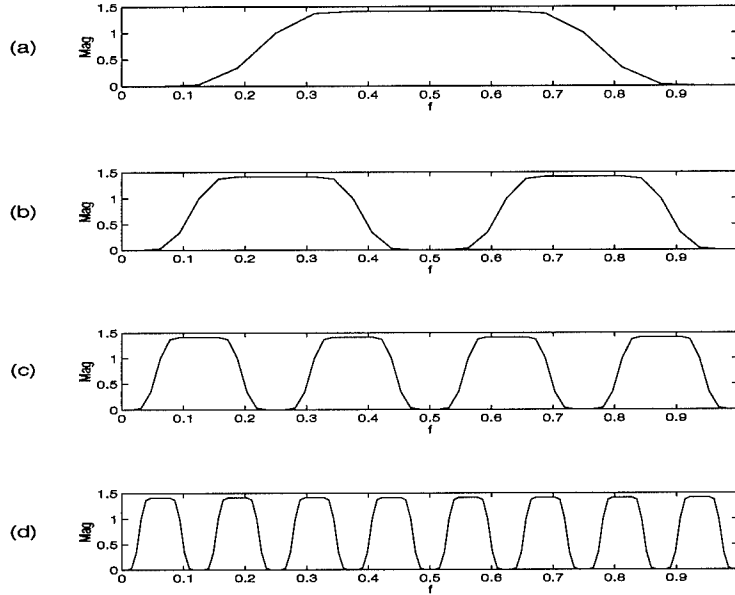


Figure 18. High Pass Filter for Various Vector Lengths. (a) Prototype Filter. (b) Vector Length of 2. (c) Vector Length of 4. (d) Vector Length of 8

If the signal is a low pass signal, then the optimum choice of vector length will always be $N = 1$. This is shown by figure 18a, where the filter with the least low frequency content is the prototype filter. Any choice of $N > 1$ will shift sections of the pass band of G toward the low frequencies and possibly increase the amount of signal energy passed through G . Since the goal is to maximize the amount of energy passed through H (and therefore minimize the amount of energy passed through G), choosing $N > 1$ can only adversely effect the energy distribution. Thus, in terms of energy redistribution, if the data signal is low pass, a multipoint multirate filter bank cannot improve data compression.

However, if the signal is band pass or high pass, a choice of decimation vector length $N \neq 1$ can significantly impact the distribution of the signal energy between subbands. For example, reference the signal and its spectrum displayed in figure 19. This signal is colored noise ranging in normalized digital frequency from 0.1 to

0.4 (where 1.0 corresponds to the Nyquist rate). If the vector decimation length is $N = 1$, a significant portion of the energy will be passed into the first high frequency decomposition level, “ $d1$ ”. This is because half of the signal energy exists at frequencies higher than the 0.25 cutoff of $G(z)$ (reference figure 18-a). For other choices of vector length ($N = 4$ or $N = 8$), less spectral energy of the signal overlaps with the expanded high pass decomposition filter $G(z^N)$ (reference figure 18c,18d).

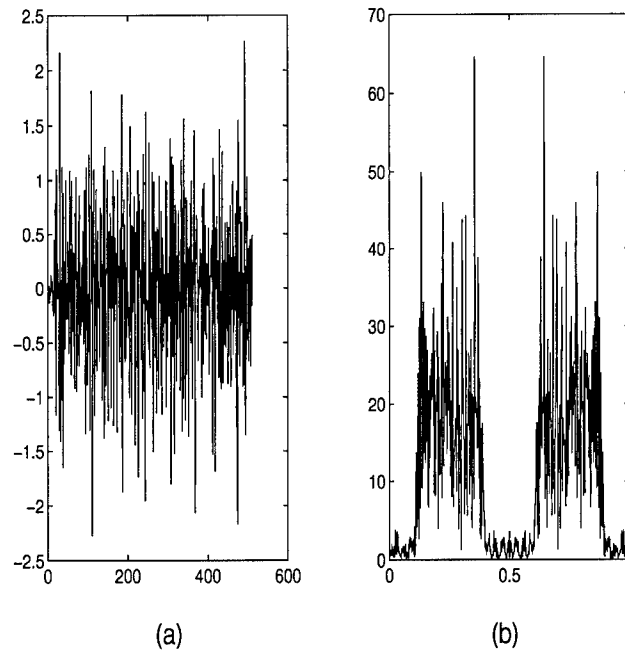


Figure 19. (a) Band Pass Signal. (b) Spectrum of Signal

At each level of the decomposition, a new vector length can be chosen which maximizes the energy pushed into the low pass subband. Figure 20 shows the distribution of energy for optimal choices of decimation vector length N compared to the traditional choice of $N = 1$ at each level.

The abscissa in figure 20 represents the high frequency fraction of the spectrum at each level of the decomposition. That is, the first half of the signal spectrum is represented by the detail coefficients $d1$, while the second half of the signal spectrum is further composed into $d2$ and $c2$. Thus, in figure 20, “0.5” corresponds to $d1$,

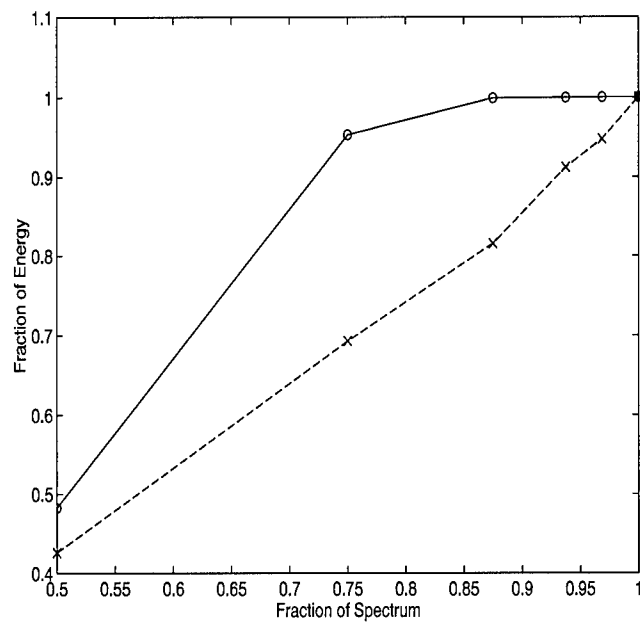


Figure 20. Energy Distribution for a Bandpass Signal. Solid line corresponds to choice of vector length $N = 1$ at each level. Dotted line corresponds to optimal choice of $N = [8, 1, 4, 8, 8]$ at each level

“0.75” corresponds to $d1 + d2$, “0.875” corresponds to $d1 + d2 + d3$, etc. The value of “1” is the entire spectrum: all the detail coefficients $d1$ to d_L , as well as the last coarse coefficients c_L .

The ordinate in figure 20 represents the fraction of signal energy present in the spectral bands. This value begins with the fraction of energy present in the detail coefficients $d1$, and increases to “1” as the fraction of the spectrum increases to “1”.

For the signal shown in figure 19, the optimal choice of N was $N = [8, 1, 4, 8, 8]$. That is, the choice of vector length $N = 8$ minimized the amount of energy passed into the first detail coefficients $d1$ (or, conversely, maximized the amount of energy passed into the first coarse coefficients $c1$). At the second level, the choice of $N = 1$ minimized the energy passed from $c1$ into $d2$. At the next levels, $N = 4$ was the best choice to minimize the energy in $d3$, and $N = 8$ was the best choice to minimize the energy in both $d4$ and $d5$ (only five levels of decomposition were performed).

Figures 21 to 35 show other test signals and the results of the energy redistribution. In figure 21, the signal is a narrow band signal which ranges in normalized digital frequency from 0.22 to 0.28. Figure 22 shows the results of the energy redistribution for the choice $N = [4, 4, 1, 8, 8]$. For this signal, the redistribution of energy to the lower bands is much better than that for the signal shown in figure 19. This is because the narrow band signal “fits” better into the nulls of the expanded comb filters $G(z^N)$.

This idea of narrow band signals fitting into the stop bands of the expanded filters is best demonstrated with a pure sinusoid (which ideally has all of its energy concentrated into one spectral line). Figure 23 shows a sinusoid and its spectrum, and figure 24 shows the results of energy redistribution. In this case, the optimal choice of vector lengths was $N = [1, 1, 8, 8, 8]$. With the conventional wavelet decomposition ($N = 1$ at each level), the energy of the signal is distributed to the subband where its frequency “naturally” falls. With optimal vector choices, the energy is entirely distributed to the coarsest decomposition level. This result will hold true for any

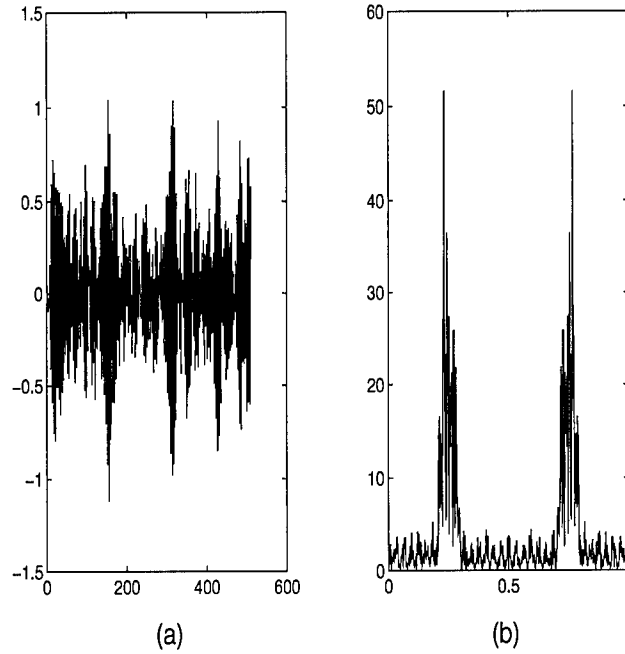


Figure 21. (a) Narrow Band Pass Signal. (b) Spectrum of Signal

sinusoid or extremely narrow band signal. Since a comb filter emphasizes certain periodicities in a signal (see section 2.1), it is possible to match a comb filter to the frequency of the sinusoidal input signal. Thus, if the decimation vector lengths N are chosen to match the frequency of the input signal, then the signal will be passed through the series of coarse decomposition comb filters to the lowest level of decomposition.

Figures 25 to 28 demonstrate the results of the energy redistribution algorithm on a low frequency band pass signal and a high pass signal. Note that the low frequency band pass signal is not low pass, but rather a band pass signal in the lower part of the spectral band. As expected, the results of energy redistribution on the low frequency band pass signal are minimal, because this signal is closely matched to the prototype low pass filter $H(z)$. However, with the high pass signal, the energy improvements are dramatic. Because the high pass signal is closely matched to the prototype high pass filter $G(z)$, any choice of vector length $N \neq 1$ (which expands

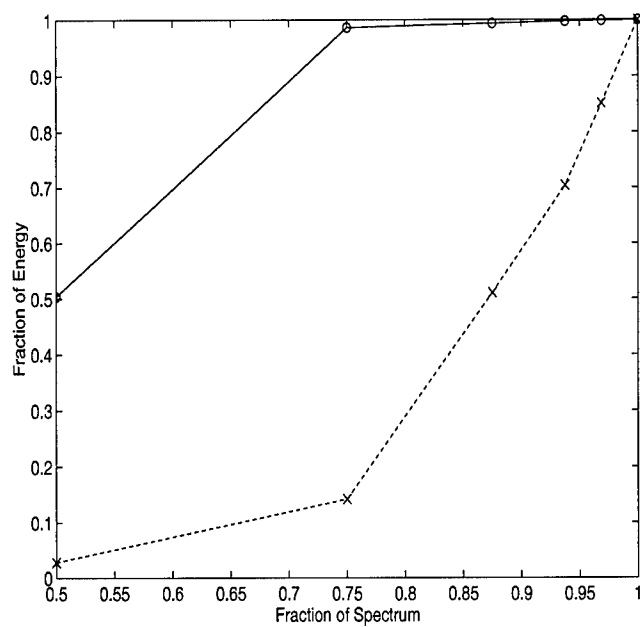


Figure 22. Energy Distribution for a Narrow Band Signal. Solid line is choice of $N = 1$ at each level. Dotted line is optimal choice of $N = [4, 4, 1, 8, 8]$ at each level

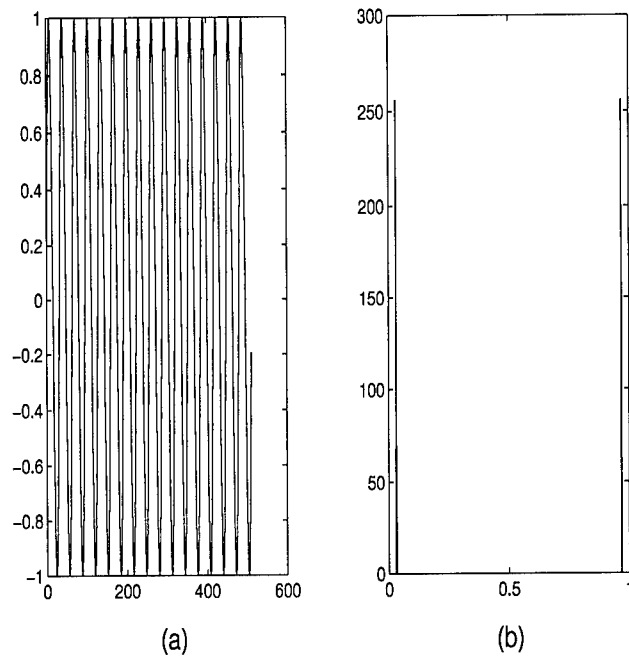


Figure 23. (a) Sinusoid Signal. (b) Spectrum of Sinusoid

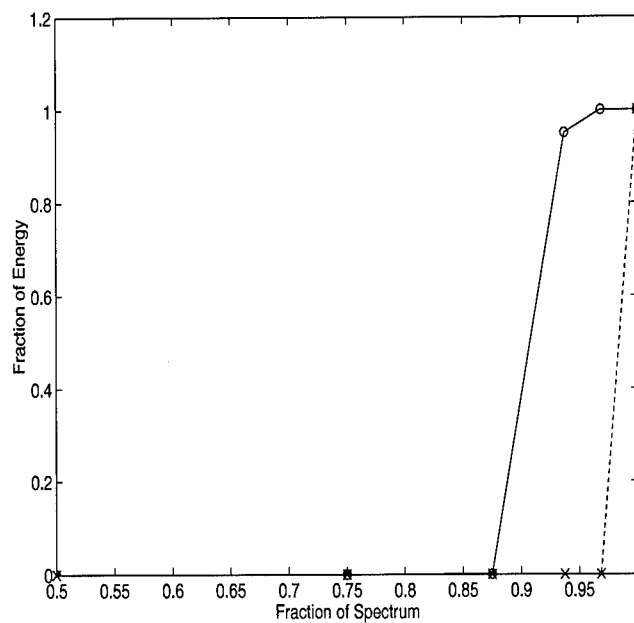


Figure 24. Energy Distribution for a Sinusoid. Solid line is choice of $N = 1$ at each level. Dotted line optimal choice of $N = [1, 1, 8, 8, 8]$ at each level

$G(z)$ and shifts portions of its pass band to lower frequencies) significantly reduces the energy passed to the detailed subbands.

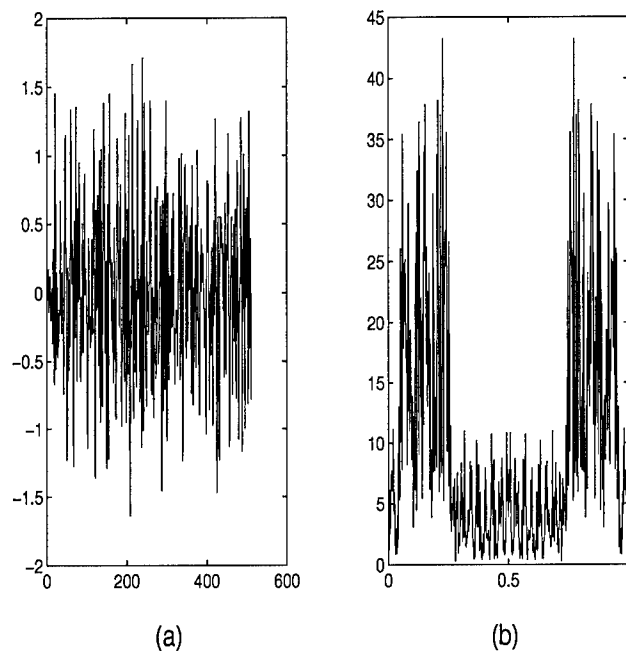


Figure 25. (a) Low Frequency Band Pass Signal. (b) Spectrum of Signal.

Figure 29 is an edge enhanced version of the common test image “Lenna”. This edge enhancement was performed by applying a high pass filter to the original image. Since edge enhancement is a common technique in digital image processing, this is a reasonable signal to process with the energy redistribution algorithm. To illustrate this energy redistribution process, consider “Lenna’s eye” as depicted in figure 30. For the purpose of this analysis, this 64×64 image is treated as a vector with length 4096. Figure 31 shows the spectrum of this signal. Although it is a relatively low frequency signal, it is still band pass. Therefore, one would expect that the energy redistribution algorithm would have a positive impact. The results of this redistribution are illustrated in figure 32, where an improvement is noted.

As an example of the processing of zero mean images, “Lenna’s eye” is considered with the mean subtracted out prior to processing. Since zero mean signals

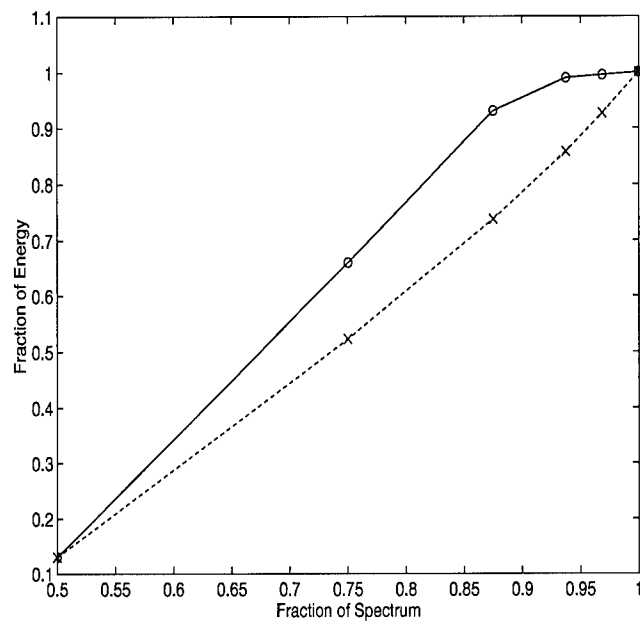


Figure 26. Energy Distribution for a Low Frequency Band Pass Signal. Solid line is choice $N = 1$ at each level. Dotted line is optimal choice of $N = [1, 8, 8, 8, 2]$

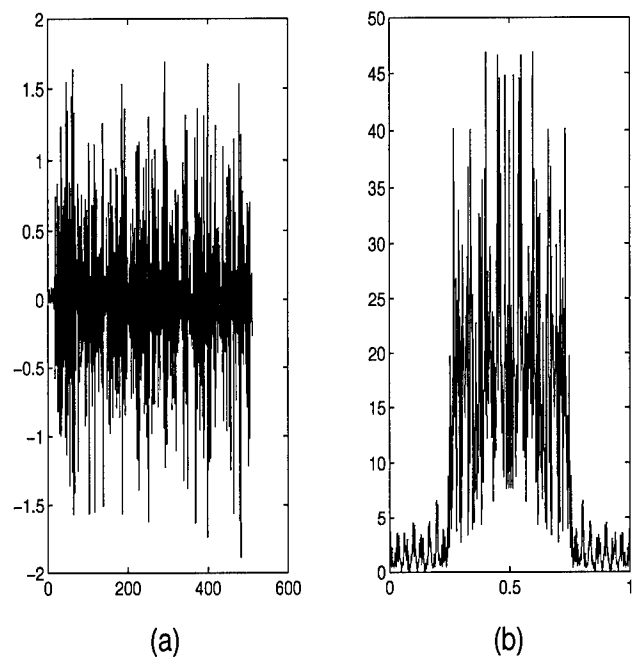


Figure 27. (a) High Pass Signal. (b) Spectrum of Signal

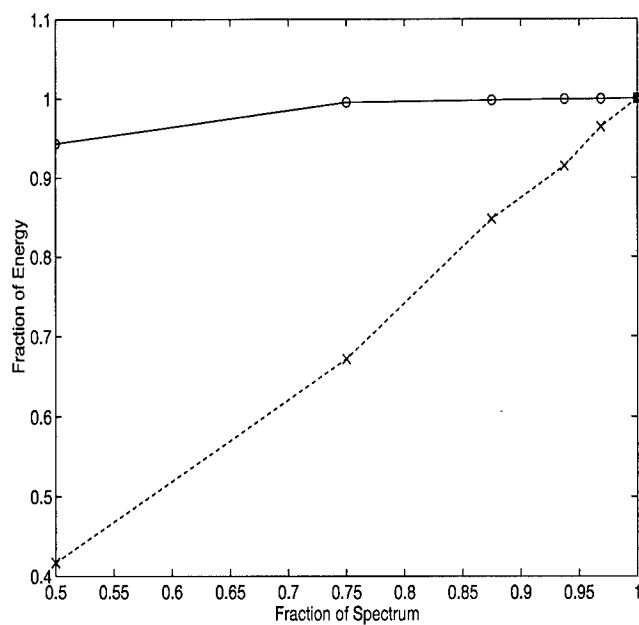


Figure 28. Energy Distribution for a High Pass Signal. Solid line is choice $N = 1$ at each level. Dotted line is optimal choice of $N = [2, 2, 4, 8, 4]$

have no energy at the lowest frequency (DC), the corresponding energy distribution improvements can be more significant, as illustrated in figure 33.

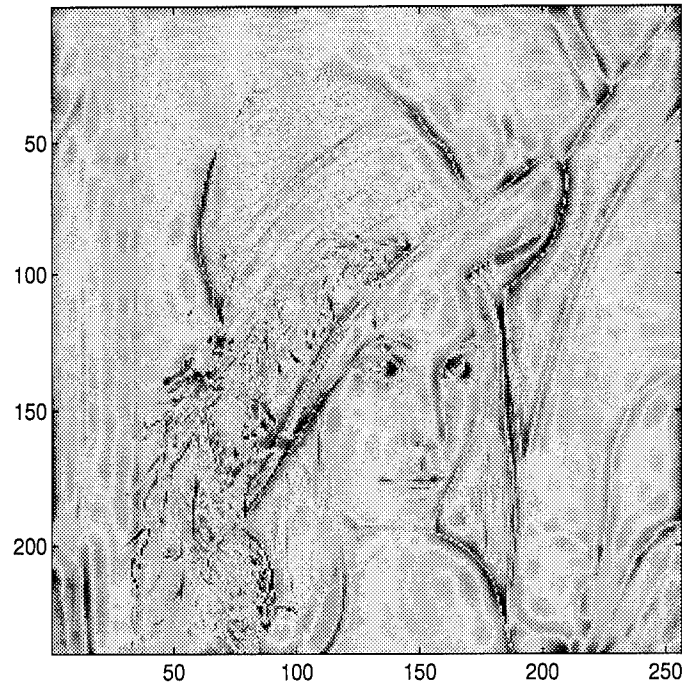


Figure 29. Lenna

Now consider the signal which is depicted in figure 34. This signal is band pass with localized narrow pass features. This signal and its spectrum are shown in figure 34. Although the signal is band pass, a significant portion of its energy is in the lower part of the spectrum. This implies that energy redistribution improvements will be minimal.

The results of the energy redistribution are shown in figure 35. There is an improvement in the distribution of the energy, but it is slight. Also, at the fourth level of decomposition, the redistributed energy is actually higher than the conventional decomposition. It is possible that, by distributing slightly more energy into the higher detail coefficients, the overall energy distribution could have been even further improved.

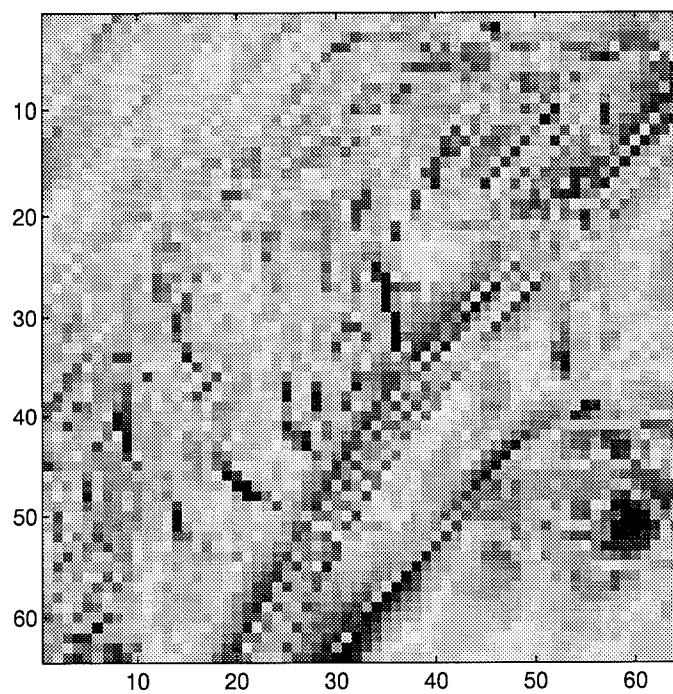


Figure 30. Lenna's Eye

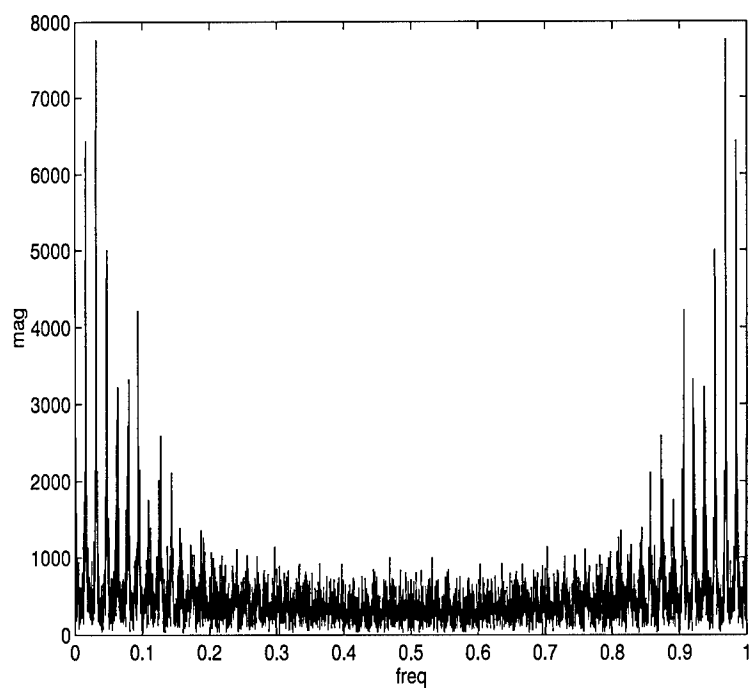


Figure 31. Spectrum of Lenna's Eye

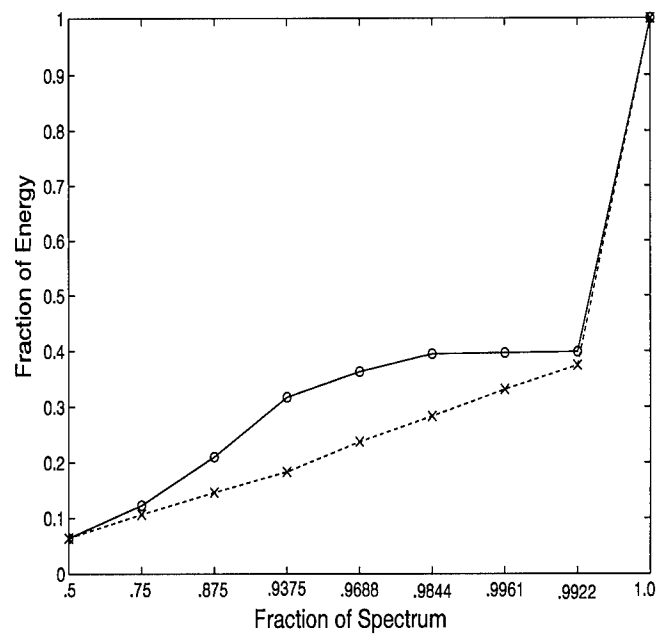


Figure 32. Energy Distribution for Lenna's Eye. Solid line is choice of $N = 1$ at each level. Dotted line is optimal choice of $N = [1, 32, 1, 16, 16, 16, 1, 8]$

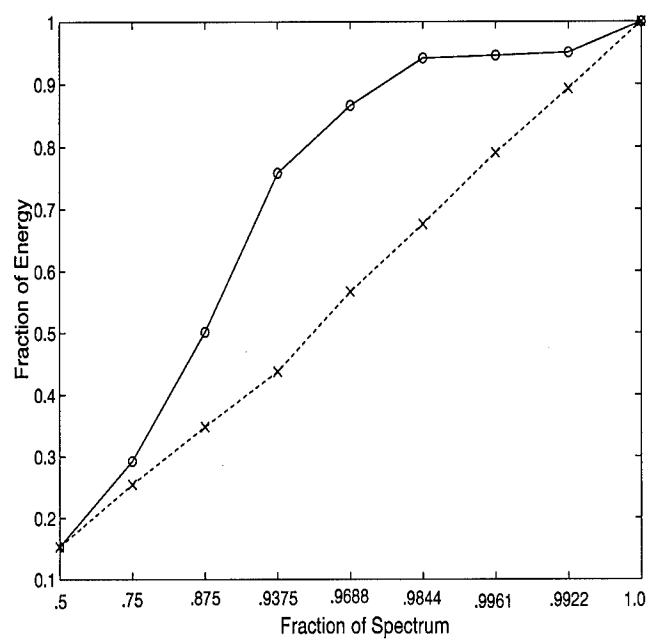


Figure 33. Energy Distribution for Lenna's Eye with Zero Mean. Solid line is choice of $N = 1$ at each level. Dotted line is optimal choice of $N = [1, 32, 1, 16, 16, 16, 1, 8]$

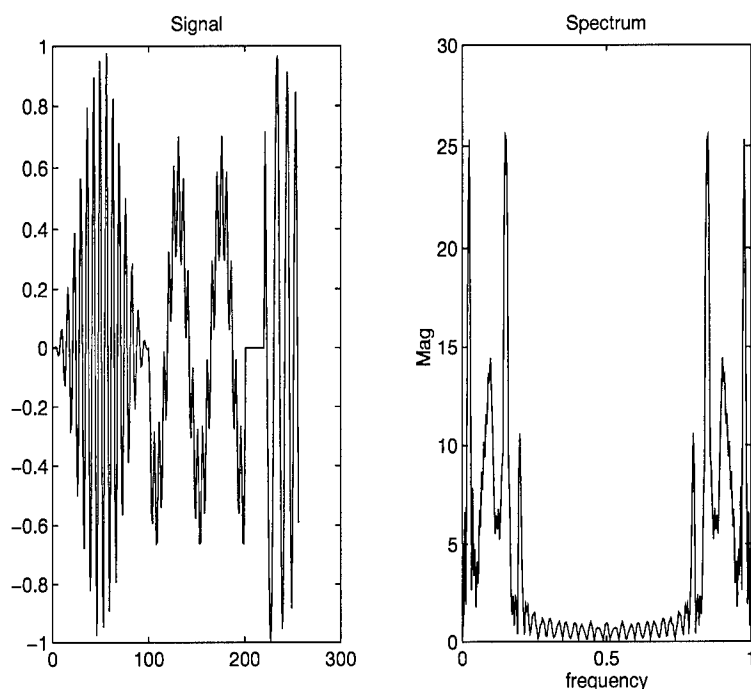


Figure 34. (a) Bandpass Signal with Narrowband Features. (b) Spectrum of Signal

4.3 Summary

Section 4.2 demonstrated the application of the multipoint wavelet decomposition algorithm to various signals. It was shown that, for band pass or high pass signals, the spectral energy of a signal can be redistributed, forcing more of the energy down to the coarse coefficients. Therefore, for this class of signals, the multipoint wavelet decomposition algorithm could be implemented as a front end to a vector quantizer, and thus used to prepare a signal for data compression.

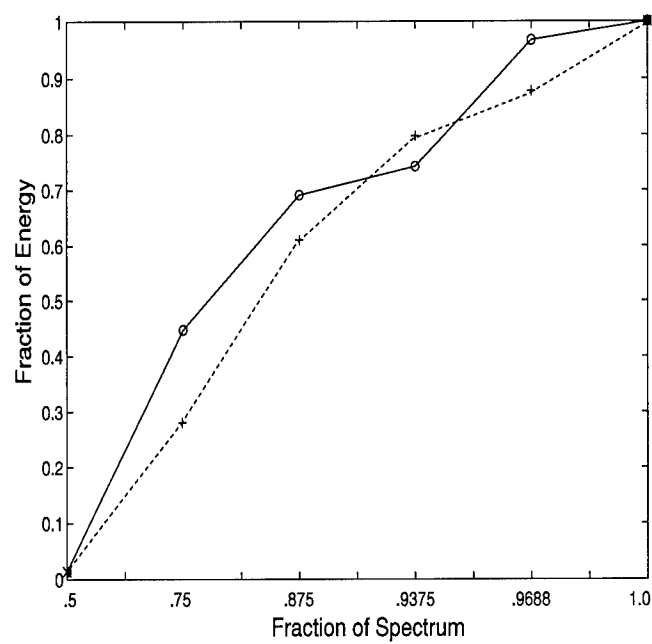


Figure 35. Energy Distribution for Bandpass Signal with Narrowpass Features. Solid line is choice $N = 1$ at each level. Dotted line is optimal choice of $N = [1, 4, 16, 8, 2]$

V. Conclusions and Recommendations for Further Study

5.1 Conclusions

This thesis provided a fundamentally new, systematic study of multipoint multirate signal processing systems. This study was accomplished by relating multipoint multirate systems to conventional multirate systems. The z-transforms of the multipoint decimator and multipoint expander were derived via equivalent circuits comprised entirely of conventional multirate operators. Proofs were presented for the basic interconnections of the multipoint operators and for the multirate noble identities. The multipoint polyphase representation was developed, and the conditions sufficient for perfect reconstruction in a multipoint multirate system were presented.

The problem of perfect reconstruction multirate filter bank design was addressed. The natural relationship of perfect reconstruction multipoint multirate systems to comb filters was shown. In addition, the concept of varying the vector lengths at each level of a generalized wavelet decomposition had never been explored prior to this thesis.

Once these theoretical foundations were established, they were then applied to a data compression feasibility study. It was clearly shown that, for band pass and high pass signals, energy can be redistributed in the corresponding multipoint multirate implementation of the wavelet decomposition. This distribution may prove useful as a front end to a vector quantizer.

5.2 Recommendations

The following recommendations are made for future research:

1. With the encouraging results of the data compression feasibility study, a vector quantizer should be developed that utilizes the multipoint multirate wavelet decomposition scheme as a front end.

2. Conditions for multirate perfect reconstruction may be equivalent to biorthogonality in the multipoint wavelet decomposition. This relationship should be explored.
3. The optimal choice of vector length at each stage of the multipoint wavelet decomposition was based on the energy distribution of the following decomposition level. A “look ahead” algorithm should be developed which chooses the decomposition vector lengths based on the overall energy distribution of the decomposition.
4. Since the theories of Multipoint Multirate Wavelet Decomposition and Vector Wavelet Decomposition were developed concurrently and independently, a comparative evaluation should be performed in the context of the data compression application.
5. Recently, Xia and Suter have shown that non-paraunitary analysis filters in a perfect reconstruction system provide additional degrees of freedom in the design of multiwavelets. With the new framework for multipoint multirate that is presented in this thesis, interesting designs may possibly be obtained if the analysis filters are not paraunitary. Thus, the design of non-paraunitary multipoint multirate analysis filters which satisfy the perfect reconstruction property should be explored.

Appendix A. The Multipoint Discrete Fourier Transform Matrix

One of the fundamental operations on multirate systems is the application of the Discrete Fourier Transform (DFT) matrix. In a single point, M channel multirate system, the data are blocked into a vector \underline{x} of length N . Then, the DFT matrix W is applied to this vector, where $[W]_{mn} = \exp(-j2\pi mn/N)/\sqrt{N}$. The resulting vector $\underline{y} = W\underline{x}$ is the Discrete Fourier Transform of \underline{x} .

In a multipoint M channel multirate system, there are two distinct methods to analyze the DFT. One can analyze the system as blocking the data into a vector \underline{x} of length MN . In this case, the DFT matrix is identical to the matrix used in a single point, MN channel multirate system.

The second method to analyze the system is to assume the data are blocked into a set of M vectors \underline{x}_i , each with length N . It would be desirable to perform DFT operations on each vector \underline{x}_i , then glue these results together in such a way that the final answer is the DFT of the total block of data (of length MN). This requires a completely new factorization of the DFT matrix.

To begin this analysis, assume that we have two blocks of data, each of length N . That is, we have a 2 channel multipoint multirate system with vector length N . Form the DFT matrix W_N . We desire a transformation T such that $T(W_N\underline{x}_0, W_N\underline{x}_1)$ is the discrete Fourier transform of the length $2N$ vector \underline{x} , where $\underline{x} = [\underline{x}_0^T \ \underline{x}_1^T]^T$. In vector form, we have

$$T(W_N\underline{x}_0, W_N\underline{x}_1) = W_{2N} \underline{x} = W_{2N} \begin{bmatrix} \underline{x}_0 \\ \underline{x}_1 \end{bmatrix}$$

We break \underline{x} up into two vectors of length $2N$, $[\underline{x}_0^T \ 0 \cdots 0]^T$ and $[0 \cdots 0 \ \underline{x}_1^T]^T$. Our system is:

$$\underline{y} = W_{2N} \left\{ \begin{bmatrix} \underline{x}_0 \\ 0 \\ \vdots \\ 0 \end{bmatrix} + \begin{bmatrix} 0 \\ \vdots \\ 0 \\ \underline{x}_1 \end{bmatrix} \right\}$$

where $\omega^k = \exp(-j2k\pi/(2N))$ and

$$W_{2N} = \frac{1}{\sqrt{2N}} \begin{bmatrix} 1 & 1 & 1 & \dots & 1 \\ 1 & \omega^1 & \omega^2 & \dots & \omega^{2N-1} \\ 1 & \omega^2 & \omega^4 & \dots & \omega^{2(2N-1)} \\ \vdots & \vdots & \vdots & \ddots & \vdots \\ 1 & \omega^{2N-1} & \omega^{2(2N-1)} & \dots & \omega^{(2N-1)^2} \end{bmatrix}$$

Since one half of each of the vectors operated on by W_{2N} is zero, when W_{2N} is distributed over the vectors, half of W_{2N} can be eliminated for each vector as follows:

$$\underline{y} = \frac{1}{\sqrt{2N}} \{ W'_{2N} \underline{x}_0 + W''_{2N} \underline{x}_1 \}$$

where

$$W'_{2N} = \begin{bmatrix} 1 & 1 & \dots & 1 \\ 1 & \omega^1 & \dots & \omega^{N-1} \\ 1 & \omega^2 & \dots & \omega^{2(N-1)} \\ \vdots & \vdots & \ddots & \vdots \\ 1 & \omega^{2N-1} & \dots & \omega^{(2N-1)(N-1)} \end{bmatrix}$$

and

$$W''_{2N} = \begin{bmatrix} 1 & 1 & \dots & 1 \\ \omega^N & \omega^{N+1} & \dots & \omega^{2N-1} \\ \omega^{2(N)} & \omega^{2(N+1)} & \dots & \omega^{2(2N-1)} \\ \vdots & \vdots & \ddots & \vdots \\ \omega^{(2N-1)(N)} & \omega^{(2N-1)(N+1)} & \dots & \omega^{(2N-1)^2} \end{bmatrix}$$

These two halves of W_{2N} can be manipulated by a row swapping matrix E_{2N} into the following form:

$$\underline{y} = E_{2N}^{-1} \left\{ \begin{bmatrix} W_N \\ W_N \begin{bmatrix} 1 & 0 \\ & \ddots \\ 0 & \omega^{N-1} \end{bmatrix} \end{bmatrix} \underline{x}_0 + \begin{bmatrix} W_N \\ \omega^N W_N \begin{bmatrix} 1 & 0 \\ & \ddots \\ 0 & \omega^{N-1} \end{bmatrix} \end{bmatrix} \underline{x}_1 \right\}$$

Thus, the problem of taking a $2N$ -point Discrete Fourier Transform breaks down into four N -point Discrete Fourier Transforms. This break down can be continued to even smaller point DFT's, resulting in the tree structure shown in figure 36.

This tree shows the case for $M = 8$. Only the individual transforms in bold type must be computed. The normal font transforms result from the addition and row swapping of results from the lower levels.

If these transforms are implemented with Fast Fourier Transforms (FFT), then the cost for an N -point transform is $5N \log N$ FLOPS and the cost for an N -point exponential weighting is $6N$ FLOPS [21]. Thus, by breaking an N -point transform into its four $(N/2)$ -point transforms, the cost is increased from $5N \log N$ to $10N \log N - 4N$. For large N , this is an increase of almost a factor of 2. If the N -point transform is broken down to k levels (the smallest transform is $N/2^k$), then the total cost will

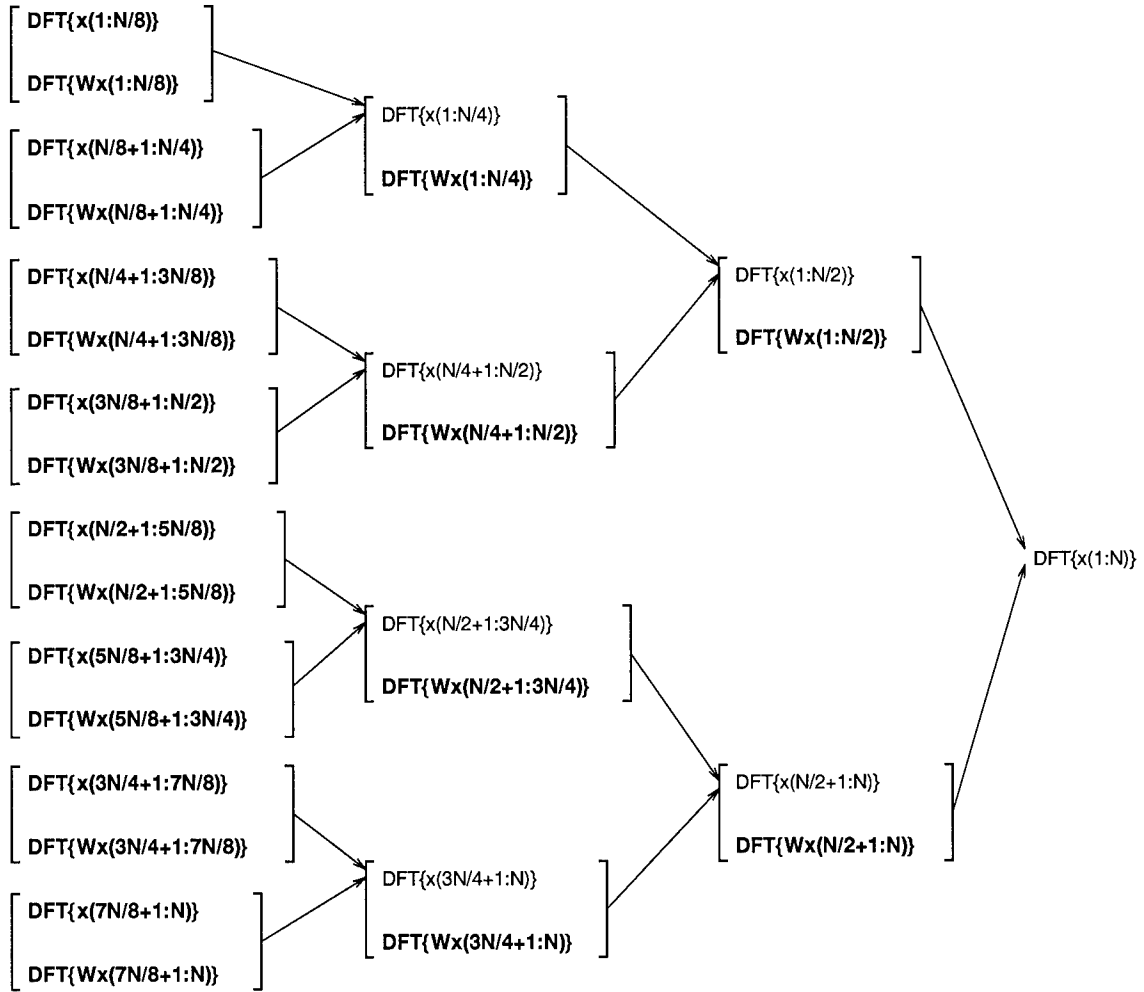


Figure 36. DFT Tree

be on the order of $5kN\log N$. This will approach $5N(\log N)^2$. Thus, this method of computing the N -point Discrete Fourier Transform is much less efficient than the N -point FFT, although this method is significantly cheaper than a direct application of the DFT matrix (which would require on the order of N^2 FLOPS).

However, the advantage of this method is that the intermediate steps provide complete Discrete Fourier Transforms on small blocks of the data. With the FFT, the intermediate results have no meaning in this way. Thus, for an increase in complexity of at worst $\log N$, frequency information is gained on all the smaller blocks at each level of the tree. This information may be worth the cost, depending on the application. Additionally, when computing the FFT, all the data must be gathered before the computation can begin. With the method described above, the computation can begin as soon as the smallest block of data is gathered. Thus, this method will have throughput advantages over the FFT (although, if only the final N -point transform is required, nothing will be more efficient than the FFT).

Appendix B. Sufficient Conditions for Perfect Reconstruction in Multipoint Multirate Systems

In section 3.1.11, it was stated that the sufficient conditions on $P(z)$ for perfect reconstruction in the multipoint multirate system are given by

$$P(z) = cz^{-m_0} \begin{bmatrix} \mathbf{0} & I_{M-r} \\ z^{-1}I_r & \mathbf{0} \end{bmatrix} \otimes \delta_{\mathbf{N}_{ij}}$$

where c is any scalar, m_0 is an integer, and $0 \leq r \leq M - 1$.

However, proof was only supplied for the case of $r = 0$ and $i = j$. The more general proof is provided here.

The output of the multipoint multirate system is given by

$$\hat{X}(z) = \sum_{k=0}^{MN-1} z^{-(MN-1-k)} \left(\sum_{m=0}^{N-1} z^{-m} \left(\sum_{l=0}^{MN-1} P_{kl}(z^{MN}) \mathcal{E}(m, l, z^{MN}) \right) \right)$$

where

$$\mathcal{E}(m, l, z) = \begin{cases} E_{m-l}(z) & l \leq m \leq N-1 \\ z^{-1}E_{m+MN-l}(z) & 0 \leq m \leq l-1 \end{cases}$$

and the $E_k(z)$ are the NM polyphase components of the original input signal $X(z)$.

In the expression for $P(z)$, let $i = i_0$ and $j = j_0$ be the indices where $\delta_{\mathbf{N}_{ij}}$ is non zero. Let $i_0 = j_0 + \gamma_0$. If

$$P(z) = \begin{bmatrix} \mathbf{0} & I_{M-r} \\ z^{-1}I_r & \mathbf{0} \end{bmatrix} \otimes \delta_{\mathbf{N}_{i_0j_0}}$$

then $P(z)$ can be partitioned as in figure 37.

For the system to exhibit perfect reconstruction, each of the MN polyphase components of the input signal must appear in the output, each expanded by MN ,

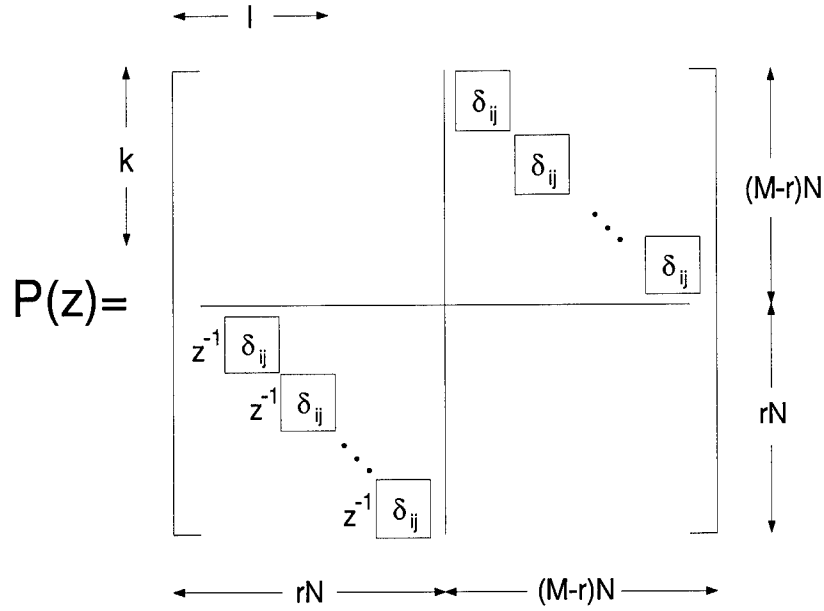


Figure 37. Partitioning of $P(z)$

multiplied by the same non-zero constant c , and each delayed by $z^{-(q+\alpha)}$, where $\alpha \in \{0, 1, \dots, MN-1\}$ is the index to the MN polyphase components of $X(z)$ and q is a non-negative integer. That is, for perfect reconstruction, $\hat{X}(z)$ must be given by

$$\hat{X}(z) = cz^{-q} \sum_{\alpha=0}^{MN-1} z^{-\alpha} E_{\alpha}(z^{MN})$$

With the partitioning of $P(z)$ shown in figure 37, there are two cases to analyze. They are:

1. $0 \leq k \leq (M-r)N-1$
2. $(M-r)N \leq k \leq MN-1$,

When, $0 \leq k \leq (M-r)N-1$, the non-zero entries of $P(z)$ are equal to one and are indexed by

$$\begin{aligned} k &= j_0 + \beta N \\ l &= Nr + i_0 + \beta N \end{aligned}$$

where $\beta \in \{0, 1, \dots, M - r - 1\}$.

Substituting in $j_0 = i_0 + \gamma_0$, these constraints become

$$\begin{aligned} l &= Nr + k + \gamma_0 \\ 0 &\leq k \leq (M - r)N - 1 \\ P_{k,l}(z) &= 1 \end{aligned}$$

We start with

$$\hat{X}(z) = \sum_{k=0}^{MN-1} z^{-(MN-1-k)} \left(\sum_{m=0}^{N-1} z^{-m} \left(\sum_{l=0}^{MN-1} P_{kl}(z^{MN}) \mathcal{E}(m, l, z^{MN}) \right) \right)$$

Pick a value of $\alpha \in \{0, 1, \dots, MN - 1\}$, then set m and l such that

$$\mathcal{E}(m, l, z) = \begin{cases} E_{m-l}(z) & l \leq m \leq N - 1 \\ z^{-1} E_{m+MN-l}(z) & 0 \leq m \leq l - 1 \end{cases}$$

reduces to $E_\alpha(z)$ or $z^{-1} E_\alpha(z)$. Thus, when $l \leq m \leq N - 1$, we have $m - l = \alpha$ and

$\mathcal{E}(m, l, z) = E_\alpha(z)$. In this case, our expression for $\hat{X}(z)$ becomes:

$$\begin{aligned} \hat{X}(z) &= \sum_{k=0}^{MN-1} z^{-(MN-1-k)} \left(\sum_{m=0}^{N-1} z^{-m} \left(\sum_{l=0}^{MN-1} P_{kl}(z^{MN}) \mathcal{E}(m, l, z^{MN}) \right) \right) \\ &= \sum_{k=0}^{MN-1} z^{-(MN-1-k)} \left(z^{-(l+\alpha)} \left(\sum_{l=0}^{MN-1} P_{kl}(z^{MN}) E_\alpha(z^{MN}) \right) \right) \\ &= \sum_{k=0}^{MN-1} \sum_{l=0}^{MN-1} P_{kl} z^{-(MN-1-k+l+\alpha)} E_\alpha(z^{MN}) \end{aligned}$$

But $l = k + \gamma_0 + Nr$, so we have

$$\begin{aligned} \hat{X}(z) &= \sum_{k=0}^{MN-1} \sum_{l=0}^{MN-1} P_{kl} z^{-(MN-1-k+l+\alpha)} E_\alpha(z^{MN}) \\ &= \sum_{k=0}^{MN-1} \sum_{l=0}^{MN-1} P_{k, k+\gamma_0-Nr} z^{-(MN-1-k+k+\gamma_0+Nr+\alpha)} E_\alpha(z^{MN}) \end{aligned}$$

$$\begin{aligned}
&= \sum_{k=0}^{(M-r)N-1} z^{-((M+r)N-1+\gamma_0+\alpha)} E_{\alpha}(z^{MN}) \\
&= (\mathbf{M} - \mathbf{r}) \mathbf{z}^{-((\mathbf{M}+\mathbf{r})\mathbf{N}-1+\gamma_0)} \mathbf{z}^{-\alpha} \mathbf{E}_{\alpha}(\mathbf{z}^{\mathbf{MN}})
\end{aligned}$$

Now, the second subcase is $0 \leq m \leq l-1$, in which case $m = \alpha + l - MN$ and $\mathcal{E}(m, l, z) = z^{-1} E_{\alpha}(z)$. The expression for $\hat{X}(z)$ becomes

$$\begin{aligned}
\hat{X}(z) &= \sum_{k=0}^{MN-1} z^{-(MN-1-k)} \left(\sum_{m=0}^{N-1} z^{-m} \left(\sum_{l=0}^{MN-1} P_{kl}(z^{MN}) \mathcal{E}(m, l, z^{MN}) \right) \right) \\
&= \sum_{k=0}^{MN-1} z^{-(MN-1-k)} z^{-(\alpha+l-MN)} \left(\sum_{l=0}^{MN-1} P_{kl}(z^{MN}) z^{-MN} E_{\alpha}(z^{MN}) \right) \\
&= \sum_{k=0}^{MN-1} \sum_{l=0}^{MN-1} z^{-(MN-1-k_{\alpha}+l)} P_{kl}(z^{MN}) E_{\alpha}(z^{MN})
\end{aligned}$$

But $l = k + \gamma_0 + Nr$, so we have

$$\begin{aligned}
\hat{X}(z) &= \sum_{k=0}^{MN-1} \sum_{l=0}^{MN-1} z^{-(MN-1-k_{\alpha}+l)} P_{kl}(z^{MN}) E_{\alpha}(z^{MN}) \\
&= \sum_{k=0}^{MN-1} z^{-(MN-1-k+\alpha+k+\gamma_0+Nr)} P_{k,k+\gamma_0+Nr}(z^{MN}) E_{\alpha}(z^{MN}) \\
&= \sum_{k=0}^{MN-1} z^{-(MN-1+\alpha+\gamma_0+Nr)} P_{k,k+\gamma_0+Nr}(z^{MN}) E_{\alpha}(z^{MN}) \\
&= \sum_{k=0}^{(M-r)N-1} z^{-(MN-1+\alpha+\gamma_0+Nr)} E_{\alpha}(z^{MN}) \\
&= (\mathbf{M} - \mathbf{r}) \mathbf{z}^{-((\mathbf{M}+\mathbf{r})\mathbf{N}-1+\gamma_0)} \mathbf{z}^{-\alpha} \mathbf{E}_{\alpha}(\mathbf{z}^{\mathbf{MN}})
\end{aligned}$$

This is the same result derived above for the case $l \leq m \leq N-1$. Thus, for any $\alpha \in \{0, 1, \dots, MN-1\}$, when $0 \leq k \leq (M-r)N-1$, the output of the system is given by

$$\hat{\mathbf{X}}(\mathbf{z}) = (\mathbf{M} - \mathbf{r}) \mathbf{z}^{-((\mathbf{M}+\mathbf{r})\mathbf{N}-1+\gamma_0)} \mathbf{z}^{-\alpha} \mathbf{E}_{\alpha}(\mathbf{z}^{\mathbf{MN}})$$

Now, we move on to the second major case, where $(m-r)N \leq k \leq M-1$, $l = k - (M-r)N + \gamma_0$, and $P_{kl}(z) = z^{-1}$. Again, there are two subcases: $l \leq m \leq N-1$ and $0 \leq m \leq l-1$.

In the first subcase, $\mathcal{E}(m, l, z) = E_\alpha(z)$ and the expression for $\hat{X}(z)$ is

$$\begin{aligned}\hat{X}(z) &= \sum_{k=0}^{MN-1} z^{-(MN-1-k)} \left(\sum_{m=0}^{N-1} z^{-m} \left(\sum_{l=0}^{MN-1} P_{kl}(z^{MN}) \mathcal{E}(m, l, z^{MN}) \right) \right) \\ &= \sum_{k=0}^{MN-1} z^{-(MN-1-k)} \left(z^{-(l+\alpha)} \left(\sum_{l=0}^{MN-1} P_{kl}(z^{MN}) E_\alpha(z^{MN}) \right) \right) \\ &= \sum_{k=0}^{MN-1} \sum_{l=0}^{MN-1} z^{-(MN-1-k+l+\alpha)} E_\alpha(z^{MN}) P_{kl}(z^{MN})\end{aligned}$$

But $l = k - (M-r)N + \gamma_0$, so we have

$$\begin{aligned}\hat{X}(z) &= \sum_{k=0}^{MN-1} \sum_{l=0}^{MN-1} z^{-(MN-1-k+l+\alpha)} E_\alpha(z^{MN}) P_{kl}(z^{MN}) \\ &= \sum_{k=0}^{MN-1} z^{-(MN-1-k+k+\gamma_0-(M-r)N+\alpha)} E_\alpha(z^{MN}) P_{k, k-(M-r)N+\gamma_0}(z^{MN}) \\ &= \sum_{k=0}^{MN-1} z^{-(-1+\gamma_0+rN+\alpha)} E_\alpha(z^{MN}) P_{k, k-(M-r)N+\gamma_0}(z^{MN}) \\ &= \sum_{k=0}^{MN-1} z^{-(-1+\gamma_0+rN+\alpha)} E_\alpha(z^{MN}) \\ &= \sum_{k=0}^{MN-1} z^{-(MN-1+\gamma_0+rN+\alpha)} E_\alpha(z^{MN}) \\ &= \sum_{k=(M-r)N}^{MN-1} z^{-((M+r)N-1+\gamma_0+\alpha)} E_\alpha(z^{MN}) \\ &= \mathbf{r} \mathbf{z}^{-((M+r)N-1+\gamma_0)} \mathbf{z}^{-\alpha} \mathbf{E}_\alpha(\mathbf{z}^{MN})\end{aligned}$$

Finally, we have the last subcase with $(M-r)N \leq k \leq MN-1$, $l = k - (M-r)N + \gamma_0$, $0 \leq m \leq l-1$, $\mathcal{E}(m, l, z) = E_\alpha(z)z^{-1}$, and our expression for $\hat{X}(z)$

becomes

$$\begin{aligned}
\hat{X}(z) &= \sum_{k=0}^{MN-1} z^{-(MN-1-k)} \left(\sum_{m=0}^{N-1} z^{-m} \left(\sum_{l=0}^{MN-1} P_{kl}(z^{MN}) \mathcal{E}(m, l, z^{MN}) \right) \right) \\
&= \sum_{k=0}^{MN-1} z^{-(MN-1-k)} \sum_{l=0}^{MN-1} z^{-(\alpha+l-MN)} P_{kl}(z^{MN}) E_{\alpha}(z^{MN}) z^{-(MN)} \\
&= \sum_{k=0}^{MN-1} \sum_{l=0}^{MN-1} z^{-(MN-1-k+\alpha+l-MN+MN)} P_{kl}(z^{MN}) E_{\alpha}(z^{MN}) \\
&= \sum_{k=0}^{MN-1} \sum_{l=0}^{MN-1} z^{-(MN-1-k+\alpha+l)} P_{kl}(z^{MN}) E_{\alpha}(z^{MN})
\end{aligned}$$

But $l = k - (M - r)N + \gamma_0$. Thus, we have

$$\begin{aligned}
\hat{X}(z) &= \sum_{k=0}^{MN-1} \sum_{l=0}^{MN-1} z^{-(MN-1-k+\alpha+l)} P_{kl}(z^{MN}) E_{\alpha}(z^{MN}) \\
&= \sum_{k=0}^{MN-1} z^{-(MN-1-k+\alpha+k-(M-r)N+\gamma_0)} P_{k, k-(M-r)N+\gamma_0}(z^{MN}) E_{\alpha}(z^{MN}) \\
&= \sum_{k=0}^{MN-1} z^{-(-1+\alpha+rN+\gamma_0)} z^{-MN} E_{\alpha}(z^{MN}) \\
&= \sum_{k=(M-r)N}^{MN-1} z^{-(MN-1+\alpha+rN+\gamma_0)} E_{\alpha}(z^{MN}) \\
&= \mathbf{r} \mathbf{z}^{-((M+r)N-1+\gamma_0)} \mathbf{z}^{-\alpha} \mathbf{E}_{\alpha}(\mathbf{z}^{MN})
\end{aligned}$$

Thus, for any $\alpha \in \{0, 1, \dots, MN - 1\}$, when $(M - r)N \leq k \leq MN - 1$, the output of the system is given by

$$\hat{\mathbf{X}}(\mathbf{z}) = \mathbf{r} \mathbf{z}^{-((M+r)N-1+\gamma_0)} \mathbf{z}^{-\alpha} \mathbf{E}_{\alpha}(\mathbf{z}^{MN})$$

Combining this with the output for $0 \leq k \leq (M - r)N - 1$, the total output of the system for a particular polyphase component $E_{\alpha}(z)$ is given by

$$\hat{\mathbf{X}}(\mathbf{z}) = \mathbf{M} \mathbf{z}^{-((M+r)N-1+\gamma_0)} \mathbf{z}^{-\alpha} \mathbf{E}_{\alpha}(\mathbf{z}^{MN})$$

Let $q = ((M + r)N - 1 + \gamma_0)$, and let $c = M$. The complete output of the multipoint multirate system is now given by

$$\hat{X}(z) = cz^{-q} \sum_{\alpha=0}^{MN-1} z^{-\alpha} E_{\alpha}(z^{MN})$$

where c is a constant, q is a non-negative integer, and the system satisfies the perfect reconstruction property.

Bibliography

1. Maurice Bellanger, Georges Bonnerot, and Michel Coudreuse, "Digital Filtering by Polyphase Network: Application to Sample Rate Alteration and Filter Banks", *IEEE Transactions on Acoustics, Speech, and Signal Processing*, Vol. 24, No. 2, pp 109-114, April 1976.
2. Ronald E. Crochiere and Lawrence R. Rabiner, Multirate Digital Signal Processing, Englewood Cliffs, NJ: Prentice Hall, 1983.
3. Ingrid Daubechies, Ten Lectures on Wavelets, Society for Industrial and Applied Mathematics, April 1992.
4. Igor Djokovic and Perinkolam P. Vaidyanathan, "Results on Biorthogonal Filter Banks", *Applied and Computational Harmonic Analysis*, Vol. 1, No. 4, pp 329-343, September 1994.
5. Gianpaolo Evangelista, "Comb and Multiplexed Wavelet Transforms and Their Applications to Signal Processing", *IEEE Transactions on Signal Processing*, Vol. 42, No. 2, pp 292-303, February 1994.
6. Masoud R. K. Khansari and Alberto Leon-Garcia, "Subband Decomposition of Signals with Generalized Sampling", *IEEE Transactions on Signal Processing*, Vol. 41, No. 12, pp 3365-3376, December 1993.
7. Weiping Li, "Image Coding Using Vector Filter Bank and Vector Quantization", *1994 IEEE International Symposium on Circuits and Systems*, Vol. 3, pp 133-136, June 1994.
8. Weiping Li, "Vector Transform and Image Coding", *IEEE Transactions on Circuits and Systems for Video Technology*, Vol. 1, No. 4, pp 297-307, December 1991.
9. Weiping Li, "On Vector Transformation", *IEEE Transactions on Signal Processing*, Vol. 41, No. 11, pp 3114-3126, November 1993.
10. Stephane G. Mallat, "Multiresolution Approximation and Wavelet Orthonormal Bases of $L^2(R)$ ", *Transactions of American Mathematics Society*, Vol. 315, No. 1, pp 69-87, September 1989.
11. Fred Mintzer, "Filters for Distortion-Free Two-Band Multirate Filter Banks", *IEEE Transactions on Acoustics, Speech and Signal Processing*, Vol. 33, No. 3, pp 626-630, June 1985.
12. Mark J. Shensa, "The Discrete Wavelet Transform: Wedding the À Trous and Mallat Algorithms", *IEEE Transactions on Signal Processing*, Vol. 40, No. 10, pp 2464-2482, October 1992.
13. Mark J.T. Smith and Thomas P. Barnwell III, "Exact Reconstruction Techniques for Tree-Structured Subband Coders", *IEEE Transactions on Acoustics, Speech and Signal Processing*, Vol. 34, No. 3, pp 434-441, June 1986.

14. Anand K. Soman and Perinkolam P. Vaidyanathan, "On Orthonormal Wavelets and Paraunitary Filter Banks", *IEEE Transaction on Signal Processing*, Vol. 41, No. 3, pp 1170-1183, March 1993.
15. Bruce W. Suter et al, "On Discrete Multiwavelet Transforms", Pre-Print, November 1994.
16. Bruce W. Suter and Xiang-Gen Xia, "Vector-Valued Wavelets and Vector Filter Banks", Pre-Print, July 1994.
17. Perinkolam P. Vaidyanathan, "Multirate Digital Filters, Filter Banks, Polyphase Networks, and Applications: A Tutorial", *Proceedings of the IEEE*, Vol. 78, No. 1, pp 56-93, January 1990.
18. Perinkolam P. Vaidyanathan and Sanjit K. Mitra, "Polyphase Networks, Block Digital Filtering, LPTV Systems, and Alias-Free QMF Banks: A Unified Approach Based on Pseudocirculants", *IEEE Transactions on Acoustics, Speech, and Signal Processing*, Vol. 36, No. 3, pp 381-391, March 1988.
19. Perinkolam P. Vaidyanathan, Multirate Systems and Filter Banks, Englewood Cliffs, NJ: Prentice Hall, 1993.
20. Perinkolam P. Vaidyanathan and Vincent C. Liu, "Efficient Reconstruction of Band-Limited Sequences from Non-uniformly decimated versions by use of Polyphase Filter Banks", *IEEE Transactions on Acoustics, Speech, and Signal Processing*, Vol. 38, No. 11, pp 1927-1936, November 1990.
21. Charles Van Loan, Computational Frameworks for the Fast Fourier Transform, Society for Industrial and Applied Mathematics, Philadelphia, PA, 1992.
22. Martin Vetterli, "A Theory of Multirate Filter Banks", *IEEE Transactions on Acoustics, Speech, and Signal Processing*, Vol. 35, No. 3, pp 356-372, March 1987.
23. Xiang-Gen Xia and Bruce W. Suter, "Multirate Filter Banks with Block Sampling", Pre-Print, April 1994.

Vita

Captain Roger L. Claypoole, Jr., was born on 16 July 1967 in Kittanning, PA. He graduated salutatorian from Kittanning High School in June 1985. He graduated from the Massachusetts Institute of Technology in June 1989 with a Bachelor of Science in Electrical Engineering. Upon graduation, he accepted a commission into the United States Air Force and was assigned to Wright-Patterson Air Force Base, OH. During his four year tour at Wright-Patterson, Captain Claypoole worked as a radar and avionics engineer in the F-16 System Program Office. In May 1993, he was selected to attend the School of Engineering at the Air Force Institute of Technology, where he pursued a Masters of Science degree in Electrical Engineering. He is a member of the Eta Kappa Nu and Tau Beta Pi engineering honor societies.

Permanent address: RD#7 Box 341
Kittanning, PA 16201

REPORT DOCUMENTATION PAGE

Form Approved
OMB No. 0704-0188

Public reporting burden for this collection of information is estimated to average 1 hour per response, including the time for reviewing instructions, searching existing data sources, gathering and maintaining the data needed, and completing and reviewing the collection of information. Send comments regarding this burden estimate or any other aspect of this collection of information, including suggestions for reducing this burden, to Washington Headquarters Services, Directorate for Information Operations and Reports, 1215 Jefferson Davis Highway, Suite 1204, Arlington, VA 22202-4302, and to the Office of Management and Budget, Paperwork Reduction Project (0704-0188), Washington, DC 20503.

1. AGENCY USE ONLY (Leave blank)		2. REPORT DATE December 1994	3. REPORT TYPE AND DATES COVERED Master's Thesis	
4. TITLE AND SUBTITLE Multipoint Multirate Signal Processing			5. FUNDING NUMBERS	
6. AUTHOR(S) Roger L. Claypoole, Jr.				
7. PERFORMING ORGANIZATION NAME(S) AND ADDRESS(ES) Department of Electrical and Computer Engineering Air Force Institute of Technology 2950 P Street Wright-Patterson AFB, OH 45433-7765			8. PERFORMING ORGANIZATION REPORT NUMBER AFIT/GE/ENG/94D-02	
9. SPONSORING / MONITORING AGENCY NAME(S) AND ADDRESS(ES) Dr. Jon Sjogren Air Force Office of Scientific Research 110 Duncan Avenue, Suite B115 Bolling AFB, DC 20332			10. SPONSORING / MONITORING AGENCY REPORT NUMBER	
11. SUPPLEMENTARY NOTES				
12a. DISTRIBUTION / AVAILABILITY STATEMENT Approved for Public Release; Distribution Unlimited			12b. DISTRIBUTION CODE	
13. ABSTRACT (Maximum 200 words) This thesis provides a fundamentally new, systematic study of multipoint multirate signal processing systems. The multipoint multirate operators are analyzed via equivalent circuits comprised entirely of conventional multirate operators. Interconnections of the operators are demonstrated, and the multipoint noble identities are derived. The multipoint polyphase representation is presented, and the M channel multipoint multirate system with vector length N is presented as an MN channel multipoint polyphase system. The conditions sufficient for perfect reconstruction in the multipoint multirate system are derived. These conditions constrain the multipoint filter banks to be composed of comb filters generated from paraunitary sets of conventional filters. The perfect reconstruction multipoint multirate system is then combined with the multiresolution wavelet decomposition to form the generalized wavelet decomposition with varying vector decimation length at each level. The generalized wavelet decomposition is used as an algorithm to redistribute the energy of a signal throughout the levels of the decomposition. It is shown that, for band pass and high pass signals, significant improvements can be made in the energy distribution. It is recommended that this algorithm be studied as a front end to a vector quantizer for data compression applications.				
14. SUBJECT TERMS Multipoint, Multirate, Signal Processing, Wavelet			15. NUMBER OF PAGES 94	
			16. PRICE CODE	
17. SECURITY CLASSIFICATION OF REPORT UNCLASSIFIED	18. SECURITY CLASSIFICATION OF THIS PAGE UNCLASSIFIED	19. SECURITY CLASSIFICATION OF ABSTRACT UNCLASSIFIED	20. LIMITATION OF ABSTRACT UL	